Contents lists available at ScienceDirect

Deep-Sea Research II

The regulation of equatorial Pacific new production and pCO$_2$ by silicate-limited diatoms

Richard Dugdale [a,*], Fei Chai [b], Richard Feely [c], Chris Measures [d], Alex Parker [a], Frances Wilkerson [a]

[a] Romberg Tiburon Center for Environmental Studies, San Francisco State University, 3152 Paradise Drive, Tiburon, CA 94920, USA
[b] School of Marine Sciences, 5706 Aubert Hall University of Maine, Orono, ME 04469, USA
[c] Pacific Marine Environmental Laboratory, 7600 Sand Point Way NE, Seattle, WA 98115, USA
[d] Department of Oceanography, University of Hawaii at Manoa, 1000 Pope Road, Marine Sciences Building, Honolulu, HI 96822, USA

ARTICLE INFO

ABSTRACT

Modeling and data from the JGOFS EqPac program suggested that the eastern equatorial Pacific upwelling ecosystem includes a quasi-chemostat culture system dominated by diatoms and limited by Si(OH)$_4$ due to a low ratio of Si(OH)$_4$ to NO$_3$ in the upwelling source water, the Equatorial Undercurrent. Diatoms were hypothesized to be the major users of NO$_3$ in this system and the amount assimilated limited by the low amount of Si(OH)$_4$ available. As a consequence NO$_3$ is left in the surface waters along with unused CO$_2$. Two cruises to the eastern equatorial Pacific (EB04 and EB05) were made to test the existing hypothesis of Si(OH)$_4$ limitation, and study the roles of source concentrations of Si(OH)$_4$ and Fe, and nutrient uptake kinetics for comparison with model predictions.

Fractionated nitrogen uptake measurements showed that diatoms at times take up the major portion of the NO$_3$. Picoplankton and some phytoplankton in the > 5-μm size group carried out primarily regenerated production, i.e. NH$_4$ uptake in a grazing dominated system. Equatorial diatoms followed uptake kinetics for Si(OH)$_4$ and NO$_3$ uptake as observed in laboratory investigations of diatoms under Si(OH)$_4$ and Fe limitations. Si(OH)$_4$ uptake responded to additions of Si(OH)$_4$ on a time scale of hours in uptake kinetic experiments while NO$_3$ uptake was unaffected by added NO$_3$. The uptake of Si(OH)$_4$ varied in a narrow range on a Michaelis-Menten hyperbola of Si(OH)$_4$ uptake vs. Si(OH)$_4$ concentration, with a maximal Si(OH)$_4$ uptake rate, V'_{maxSi} set to a relatively low value by some factor(s) other than Fe on a longer time scale, i.e., days in shipboard enclosures. Simply enclosing water collected from the mid euphotic zone and incubating for some days on deck at 50% surface irradiance increased V'_{maxSi} in accordance with V'_{maxSi} being a function of incident irradiance. Fe additions to the enclosures also increased V'_{maxSi} but not to the same extent as only enclosing the water and incubating on deck. The values of V'_{maxSi} and $V'Si$ showed no relation to ambient Fe concentrations. The study was carried out in a region relatively rich in Fe, from 140°W eastward. These results call into question conclusions that Fe and Si(OH)$_4$ co-limit production based upon enclosure experiments amended with Fe and incubated at near surface irradiance without first considering what causes the initial large increase in V'_{maxSi} in the on-deck control enclosures. Some evidence for an Fe effect was seen at the eastern end of the EB04 equatorial section, where Fe concentration generally declined in the eastward direction and at about 118°W reached a low level that may have resulted in the reduction of the V'_{maxSi}. Data from the EB04 and EB05 cruises showed a close correlation between surface TCO$_2$ and NO$_3$ concentration as expected from the demonstrated limitation of diatom NO$_3$ uptake by Si(OH)$_4$, highlighting the important role of equatorial diatoms in the global carbon cycle.

1. Introduction

The equatorial Pacific is a key region of the world ocean, not only because El Niño and La Niña events are generated there, but also because the region is the largest oceanic source of CO$_2$ to the atmosphere (Feely et al., 1999a; Takahashi et al., 2002). The high values of pCO$_2$ and TCO$_2$ at the surface of the eastern equatorial Pacific (EEP) occur in concert with low concentrations of chlorophyll and relatively high concentrations of nutrients, notably nitrate (NO$_3$). The EEP has been categorized as HNLC, i.e. high-nutrient low-chlorophyll, a term applied to other regions of the world ocean that exhibit anomalously low productivity in the presence of relatively high, unused nutrients (Minas and Minas, 1992). More specifically, it has been described as high-nitrate, low-silicate

$(Si(OH)_4)$ low-chlorophyll by Dugdale et al. (1995) and Dugdale and Wilkerson (1998), who suggested that $Si(OH)_4$ may be a factor limiting new production. New production is the phytoplankton uptake of newly available nutrient in the euphotic zone, for example from vertical advection or mixing of waters from the nutricline (Dugdale and Goering, 1967).

The question "why isn't the equatorial Pacific greener?" (Barber, 1992) was responsible in part for the establishment of the US JGOFS EqPac program in the early 1990's (Murray, 1995, 1996; Murray et al., 1997). Data from the EqPac cruises provided considerable insight into the physics, chemistry and biology of the equatorial system, but left the "why isn't it greener?" question without an unequivocal answer. However, it was generally accepted on the basis of the Iron-Ex I and II open-ocean mesoscale experiments made to the east and out of the upwelling area, that low Fe was the likely cause (Coale et al., 1996). Few Fe measurements and virtually no experimental verification of Fe limitation were available for synthesis of the EqPac results. Vertical profiles of NO_3 and $Si(OH)_4$ from the EqPac data further to the west than Iron-Ex at 140°W revealed low $Si(OH)_4$ relative to NO_3 in the upwelling source water (the equatorial undercurrent, EUC) and a 1:1 $Si(OH)_4$:NO_3 disappearance ratio from source to surface waters suggesting diatoms (which require Si for frustule formation) as the only users of NO_3. Ku et al. (1995) using ^{228}Ra described low flux of $Si(OH)_4$ compared to NO_3 in equatorial upwelling waters and suggested $Si(OH)_4$ limitation of diatom productivity was likely to result.

Building on a silicate pump model that exported more $Si(OH)_4$ relative to NO_3 into deep waters (Dugdale et al., 1995), the chemostat analogy for the EUZ of Frost and Franzen (1992) and data from the US JGOFS EqPac program, Dugdale and Wilkerson (1998) constructed a model of new production for the equatorial upwelling zone/ecosystem (EUZ). NO_3 was taken up and assimilated only by the diatoms and only to the extent allowed by the $Si(OH)_4$ supply (using an assumed uptake ratio of 1:1), leaving excess NO_3 and TCO_2 at the surface. A non-diatom, small cell-sized phytoplankton group termed picoplankton used only ammonium (NH_4), i.e. regenerated nitrogen. Although the Dugdale and Wilkerson (1998) model fit the JGOFS EqPac nutrient distributions, critical variables had not been measured up to that time in the EUZ to enable verification of phytoplankton rates and species composition. These unavailable data included biomass of the diatoms as biogenic silica (BSi), $Si(OH)_4$ uptake (production) rates, the proportion of NO_3 and NH_4 flowing to the diatoms versus the picoplankton, and the kinetics of $Si(OH)_4$ and NO_3 uptake along with possible effects of Fe on $Si(OH)_4$ and NO_3 processes. Subsequently, a next generation one-dimensional Carbon, Silicon, Nitrogen Ecosystem (CoSiNE) model (Chai et al., 2002) of the equatorial upwelling system combined the Dugdale and Wilkerson (1998) model with the nitrogen based model of Chai et al. (1996). It incorporated the results of the EqPac research and proved robust when physics in the vertical dimension was included. The CoSiNE model allowed use of two forms of nitrogen (NO_3 and NH_4) by both functional phytoplankton groups (diatoms and picoplankton) and included a fixed Fe effect on photosynthesis. It successfully reproduced most of the known characteristics of the EUZ, based upon a new production system regulating on $Si(OH)_4$ through the diatom population (Chai et al., 2002; Dugdale et al., 2002; Jiang et al., 2003).

Subsequently the CoSiNE model has been transferred into a series of three-dimensional general circulation models describing both equatorial Pacific and Pacific basin physical, chemical and biological processes with considerable success (Chai et al., 2003, 2009; Jiang and Chai, 2005, 2006; Bidigare et al., 2009). Recently three-dimensional modeling work using CoSiNE has also simulated effects of Fe, and Fe addition experiments in stimulating

diatom growth in the far eastern equatorial Pacific (Chai et al., 2007). However, a number of parameters and functions in the CoSiNE model were extrapolations of data from other regions of the ocean and from culture studies. Still missing were the critical measurements for the EUZ of $Si(OH)_4$ uptake rates and kinetics, diatom biomass, cell size-fractionated NO_3 and NH_4 uptake rates, and effects of low Fe concentrations on phytoplankton processes. Two cruises to the equatorial Pacific (EB04 in December 2004 and EB05 in September 2005) were conducted to make the missing measurements, test the assumptions and functioning of the 1D (CoSiNE) model and explore possible effects of Fe on ecosystem functioning.

A preliminary analysis of the EB04 data, concentrated at 110°W, supported the Dugdale and Wilkerson (1998) diatom-chemostat model, since the size-fractionated NO_3 and NH_4 uptake measurements showed on average, 79% of NO_3 was taken up in surface waters by cells > 5-µm in size (that includes the diatoms) (Dugdale et al., 2007). Comparison of EB04 data and CoSiNE model predictions showed close agreement of surface NO_3 and $Si(OH)_4$ concentrations and reasonable agreement of N uptake rates (within two s.d. of the mean, Dugdale et al., 2007). With this new data, Dugdale et al. (2007) concluded that, from an understanding of the $Si(OH)_4$ limited, quasi-chemostat nature of the diatom productivity, "three mysteries about the equatorial Pacific upwelling ecosystem should be considered solved by this modeling and data study 1) the low chlorophyll with "high" nutrients, 2) the relatively low and invariant primary production and 3) high surface CO_2". On the basis of grow-out (deck enclosure) experiments in which $Si(OH)_4$ uptake kinetics were measured on EB05, Brzezinski et al. (2008) concluded that both Fe and $Si(OH)_4$ "regulated" the diatom productivity in the equatorial Pacific. Here we re-examine the $Si(OH)_4$ uptake and kinetic data in the dynamic setting of the ecosystem in contrast to conclusions from on-deck enclosures and reach a different conclusion, that for most of the equator from 140°W eastward to 110°W, no regulatory role for Fe was apparent in the station data. On the other hand, the $Si(OH)_4$ and NO_3 uptake kinetics and station data were in accord with the concept of a quasi-chemostat, $Si(OH)_4$ limited diatom productivity system. The sampling stations of EB05 were concentrated at 140°W that had been the focus of EqPac data used for testing the Dugdale and Wilkerson (1998) and Chai et al. (2002) CoSiNE models.

Here we present an analysis of a subset of the EB04 and EB05 data to understand regulatory mechanisms for the role of diatoms and $Si(OH)_4$ in the equatorial upwelling system and the possible role of Fe. More specifically, the use of different forms of inorganic nitrogen by different phytoplankton will be evaluated, in particular the diatom contribution to NO_3 uptake. Then using the chemostat analogy, a detailed analysis of how uptake kinetics of $Si(OH)_4$ (as a limiting nutrient) can be affected by non-limiting nutrients (Dugdale et al.,1981) and other factors, and influence the EUZ diatom growth rate and productivity processes. The availability of uptake rates and kinetics for $Si(OH)_4$ and NO_3, and oceanic concentrations of Fe in a single data set makes it possible to evaluate the potential role of Fe in these processes.

2. Materials and methods

Two cruises were made aboard the R/V Roger Revelle, EB04 (10-28 December, 2004) that sampled from east to west, from 110°W to 140°W with a latitudinal section across the equator at 110°W followed by a zonal section to 140°W (Fig. 1), and EB05 (8-24 September 2005) with a latitudinal section across the equator at 140°W, followed by zonal stations to 123.5°W (Fig. 1). Sea water was collected using either a CTD rosette (with
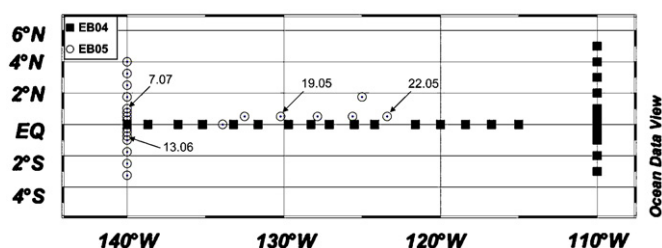
Fig. 1. Station locations for the two equatorial cruises, a) EB04 (squares), b) EB05 (open circles) with arrows that point to where "delayed kinetic" experiments were conducted.

acid-cleaned 10-L PVC Niskin bottles with Teflon coated springs) or a trace-metal clean rosette system (Brzezinski et al., 2008). Water samples from throughout the water column were collected in 20 ml polypropylene bottles, for measurement of NO_3 (measured as NO_3 plus NO_2 with consistently low NO_2) and $Si(OH)_4$ concentrations and were held at 4 °C until analysis (within 12-24 hours) with a Bran and Luebbe AutoAnalyzer II (NO_3 according to Whitledge et al., 1981 and $Si(OH)_4$ using Bran Luebbe AutoAnalyzer Applications, 1999). For NH_4 analyses, water was sampled into 60-ml polycarbonate centrifuge tubes and assayed according to Solorzano (1969) on shipboard. TCO_2 samples were analyzed using the coulometric method described by Feely et al. (1999b). Discrete water samples from vertical profiles were collected using a trace metal-clean rosette system and trace metal protocols described in Measures et al. (1995) and Kaupp et al. (2011). Aliquots for shipboard trace metal determination were filtered through 0.45-μm acid leached polysulphone membrane sandwich filters (Pall #4614) mounted in closed-face 47-mm polypropylene filter holders (GE Osmonics #1262579). The results of the dissolved Al and Fe determinations for EB04 are presented in Kaupp et al. (2011) and for EB05 (Yang et al., in prep). Rate measurements for uptake of $Si(OH)_4$, NO_3 and NH_4 were made on water sampled from depths within the euphotic zone using the CTD rosette and referred to here as station data, and on water obtained from mid-euphotic zone depths (15-30% light penetration depth) with the clean rosette and then held in 20-L carboys on deck at 50% ambient irradiance for 5 days referred to here as shipboard on-deck grow-outs or enclosures. Details of the sub sampling from the TM rosette are in Brzezinski et al. (2011). A number of other treatments/additions to the carboys were made in the grow-out series and are described elsewhere in this volume. The data included here are from a set to which germanium was added (see Krause et al., 2011) and from a set in which Fe and $Si(OH)_4$ were added to separate carboys along with a control carboy (no additions). The water in the on-deck grow-outs were sampled upon filling and after 24, 48 and 96 hours for $Si(OH)_4$ and NO_3 kinetic experiments. The results of these experiments are referred to as delayed kinetics. The four stations where these were carried out are shown by arrows in Fig. 1. The procedures for $^{32}Si(OH)_4$ uptake kinetic measurements and results are described by Brzezinski et al. (2008). NO_3 uptake kinetic measurements could not be made in the usual way by adding a series of increasing NO_3 concentrations to bottles incubated with $^{15}NO_3$ as tracer, since the ambient NO_3 concentrations were well above published K_S for NO_3 (the concentration of NO_3 at which maximal NO_3 uptake is reduced to one-half maximum). Instead, evaluation of the possible effect of increased NO_3 on the uptake of NO_3 was made by comparing the results of an incubation in which a trace addition of $^{15}NO_3$ was added, with an incubation in which 5 μM $^{15}NO_3$ (called saturated) was added. In this way an evaluation of substrate concentration effect on the maximal uptake rate of NO_3 (V'_{maxNO3}) could be made.

NO_3 and NH_4 uptake rates were measured using size fractionation of the phytoplankton after incubation with ^{15}N labeled N compounds, into the > 5-μm size fraction (using 5-μm pore sized silver filters), the total community (using GF/F filters) and the < 5-μm fraction obtained by subtraction. Water was sampled from the CTD rosette into acid-washed 2-L clear polycarbonate bottles at depths equivalent to 52, 13, and 0.8% of surface irradiance on EB04 and at all LPD's on EB05. These bottles were inoculated with either $K^{15}NO_3$ or $^{15}NH_4Cl$ (both at 99 atom% ^{15}N) at concentrations equivalent to 5-10% of ambient concentration; i.e., trace enrichments. The bottles were then placed into an on-deck water-cooled table screened to simulate collection site in situ temperature and irradiance conditions, and incubated for six daylight hours around local noon. Incubations were terminated by filtration onto pre-combusted (450 °C for 4 hours) Whatman 25-mm GF/F filters for uptake rates by the entire phytoplankton community (nominal pore size of 0.7 μm) or onto 25-mm diameter Poretics silver filters with 5-μm pore-size that sampled the larger phytoplankton cells, with cell diameters > 5-μm. All filters were kept frozen until analysis when they were dried (< 60 °C for > 24 hours) and analyzed for ^{15}N enrichment and PON with a PDZ Europa 20/20 mass spectrometer system (Wilkerson and Dugdale, 1992). The transport (ρ) and specific uptake (V) rates were calculated according to Dugdale and Wilkerson (1986). The equation relating these parameters is:

$$\rho = V*B \qquad (1)$$

where ρ is the transport rate with units of mass per unit volume per unit time (e.g. μmol l^{-1} h^{-1}), V is the biomass specific uptake rate with unit t^{-1} and B is the biomass of the specific nutrient in the phytoplankton with units μmol l^{-1}.

3. Results and discussion

First, different approaches to assess the contribution of diatoms to equatorial NO_3 uptake will be described and then the way that the $Si(OH)_4$ limited diatoms form a quasi-chemostat new production system in the EUZ will be developed.

3.1. Equator-wide estimates of NO_3 and $Si(OH)_4$ uptake

For detailed NO_3 and NH_4 uptake values measured along all the transects during EB04 and EB05 see Parker et al. (2011), and for $Si(OH)_4$ uptake see Krause et al. (2011). The average depth-integrated uptake rates for NO_3 and $Si(OH)_4$ measured at stations within 1 degree of the equator on EB04 and EB05 (i.e. 1°N to 1°S) are compared with independent estimates of these rates in Table 1. Measured ρNO_3 for the total phytoplankton community (measured with a GF/F filter, ~ 0.7-μm pore size) of 3.31 and 4.11 mmol m^{-2} d^{-1} for EB04 and EB05 are close to the values obtained from a NO_3 budget analysis based on ROMS-CoSiNE model results for both cruises by Palacz et al. (2011) calculated as 3.74 and 4.74 mmol m^{-2} d^{-1} for two different sized equatorial boxes (the Wyrtki box 5°N - 5°S, 180 - 90°W and the EEP box, 2°N - 2°S, 110 - 140°W) (Table 3 in Palacz et al., 2011). In one of their NO_3 budget calculations, Palacz et al. (2011) used the modeled annual mean velocity, combined with the modeled annual mean NO_3 concentration, which produced net physical supply of NO_3 to the euphotic zone. Then this net NO_3 supply was assumed to support the NO_3 uptake by phytoplankton groups. To estimate $\rho Si(OH)_4$, Palacz et al. (2011) used the same approach, but replaced the modeled NO_3 with the modeled annual mean $Si(OH)_4$, and obtained $Si(OH)_4$ uptake values of 2.89 and 3.70 mmol m^{-2} d^{-1} for the Wyrtki box and the EEP box, respectively (Table 3 in Palacz et al., 2011).

Table 1
Integrated measured and modeled rates and ratios of equatorial NO_3 and $Si(OH)_4$ uptake (1°N to 1°S unless otherwise noted).

Source	$\rho NO_3 T$ all cells	$\rho NO_3 < 5$-μm cells	$\rho NO_3 > 5$-μm cells	ρSi all cells	$\rho NO_3 > 5$-μm: ρSi	$\rho NO_3 T : \rho Si$
	mmol m^{-2} d^{-1}					
This study						
EB04	3.31	0.99	2.32	1.81	1.28	1.83
EB05	4.11	1.27	2.84	1.24	2.29	3.31
Palacz et al. (2011)						
5°N-5°S, 180-90°W	3.74			2.89		1.29
2°N-2°S, 110-140°W	4.74			3.70		1.28
Dugdale et al., 2002						
CoSiNE	1.96	0.97	0.86	1.65	0.52	1.11
Dugdale and Wilkerson (1998)	2.36	0	2.36	2.36	1.00	1.00
Leynaert et al. (2001)						
EBENE, 0,180°W				2.58		
Rodier and LeBorgne (1997)	2.9					
Blain et al. (1997)						
FLUPAC				2.0		

The measured values (Table 1) are higher than the CoSiNE model estimate for NO_3 uptake (1.96 mmol m^{-2} d^{-1}) (Dugdale et al., 2002), which was estimated for the entire equatorial Pacific (180 W-90°W, 5°N-5°S), but closer to the estimate of Dugdale and Wilkerson (1998) of 2.36 mmol m^{-2} d^{-1} for the same location and 2.9 mmol m^{-2} d^{-1} measured during FLUPAC at 0°, 150°W by Rodier and LeBorgne (1997). The mean measured $Si(OH)_4$ uptake rates on EB04 and EB05 of 1.81 and 1.24 mmol m^{-2} d^{-1} (Krause et al., 2011) compares well with the CoSiNE modeled value of 1.65 mmol m^{-2} d^{-1} (Dugdale et al., 2002). The higher values of 2.58 mmol m^{-2} d^{-1} measured on the EBENE cruise by Leynaert et al. (2001) at 180°W on the equator and 2.0 mmol m^{-2} d^{-1} for FLUPAC (Blain et al., 1997) are closer to those of the budget analysis by Palacz et al. (2011), 2.89 and 3.70 mmol m^{-2} d^{-1}. Considering the variety of approaches used to produce these estimates of NO_3 and $Si(OH)_4$ uptake rates, the agreement is remarkably good. The CoSiNE model estimates the $Si(OH)_4$ uptake correctly but underestimates the total NO_3 uptake ($\rho NO_3 T$) due to the lack of a non-diatom > 5-μm autotrophic group using NO_3 in the model yet observed in EB04 and EB05 (Parker et al., 2011).

3.2. Partitioning NO_3 uptake between equatorial phytoplankton groups

The proportion of diatoms making up the EUZ phytoplankton population is known to be small. In the EqPac data, diatoms were estimated as 12% of the total phytoplankton biomass by HPLC pigment analysis (Bidigare and Ondrusek, 1996) and in EB04 and EB05 the proportion of diatoms may be even smaller, as low as 6.5% of the autotrophic carbon biomass and 13 ± 8% of the > 5-μm size fraction (all diatoms were > 5-μm, Taylor et al., 2010). However the diatom contribution to the total NO_3 production has been unknown. The availability of measured $Si(OH)_4$ uptake rates along with fractionated NO_3 uptake rates on our two cruises helps to address this question directly.

Originally Dugdale and Wilkerson (1998) used the slope of NO_3:$Si(OH)_4$ concentrations in the euphotic zone to evaluate diatom NO_3 uptake. These slopes were considered as biological drawdown ratios although they may be significantly altered by *in situ* regeneration and thereby different from the uptake ratios. In plots of the upper 200 m of the water column at 140°W using

JGOFS EqPac data, the slope of the NO_3:$Si(OH)_4$ was 1:1 (Dugdale and Wilkerson, 1998), and this was used to assume all NO_3 drawdown was done by diatoms. The data set (from 0–200 m) from 1°N to 1°S for EB04 yielded two slopes for NO_3:$Si(OH)_4$ concentrations depending on the sampling depths for stations; a slope of 1.32 from surface to 200 m (Fig. 2A) and 1.55 for the samples with concentrations up to 10 μM $Si(OH)_4$, i.e. from shallower depths (Fig. 2B). Similar analysis for EB05 yielded a slope of 1.12 for the deeper values (Fig. 2C) and 2.19 using samples with concentrations up to 5 μM $Si(OH)_4$, i.e. measured near the surface (Fig. 2D).

Here we use a number of approaches/calculations, using data averaged from EB04 and EB05 stations between 1°N to 1°S (upper three LPD's, 100%, 52%, 31% LPD's), to assess the contribution of diatoms to NO_3 uptake (Table 2). If it is assumed that all the phytoplankton in the > 5-μm size class are diatoms then an upper estimate (Approach 1) of the diatom contribution to total NO_3 uptake ($\rho NO_3 T$) is simply the ρNO_3 by the > 5-μm size class (measured on the 5-μm pore-sized silver filters); 5.56 and 5.79 nmol L^{-1} h^{-1} (78.3 and 69.4% of $\rho NO_3 T$) for EB04 and EB05 respectively (Table 2). A second estimate (Approach 2) employs the slope of near surface rates of NO_3 uptake by the > 5-μm sized versus total phytoplankton community for all EB04 and EB05 stations. Parker et al. (2011) reported a regression slope of 0.87, i.e. 87% diatom NO_3 uptake to $\rho NO_3 T$ if all > 5-μm NO_3 uptake is attributed to diatoms. When this relationship (percentage) was applied to the $\rho NO_3 T$ in Table 2, NO_3 uptake estimates for the > 5-μm fraction (diatoms) were 6.17 and 7.26 nmol N L^{-1} h^{-1} for EB04 and EB05, respectively.

A third estimate used data from shipboard grow-out experiments in which germanium (+Ge) was added to inhibit $Si(OH)_4$ uptake by diatoms. To estimate the contribution of diatoms to total phytoplankton NO_3 uptake, NO_3 drawdown in control and Ge-supplemented carboys during nine grow-out experiments conducted during EB04 and EB05 are compared (Table 3). It was assumed that NO_3 drawdown in the control (ΔNO_{3cont}) would provide a good estimate of total phytoplankton NO_3 uptake during the incubation period (96 or 120 hours), while NO_3 drawdown in +Ge treatments (ΔNO_{3+Ge}) represents NO_3 uptake by the non-diatom fraction of the phytoplankton community. The fraction of the NO_3 drawdown resulting from diatom activity was calculated by difference between ΔNO_{3cont} and ΔNO_{3+Ge}. The assumption that +Ge treatments provide an estimate of non-diatom
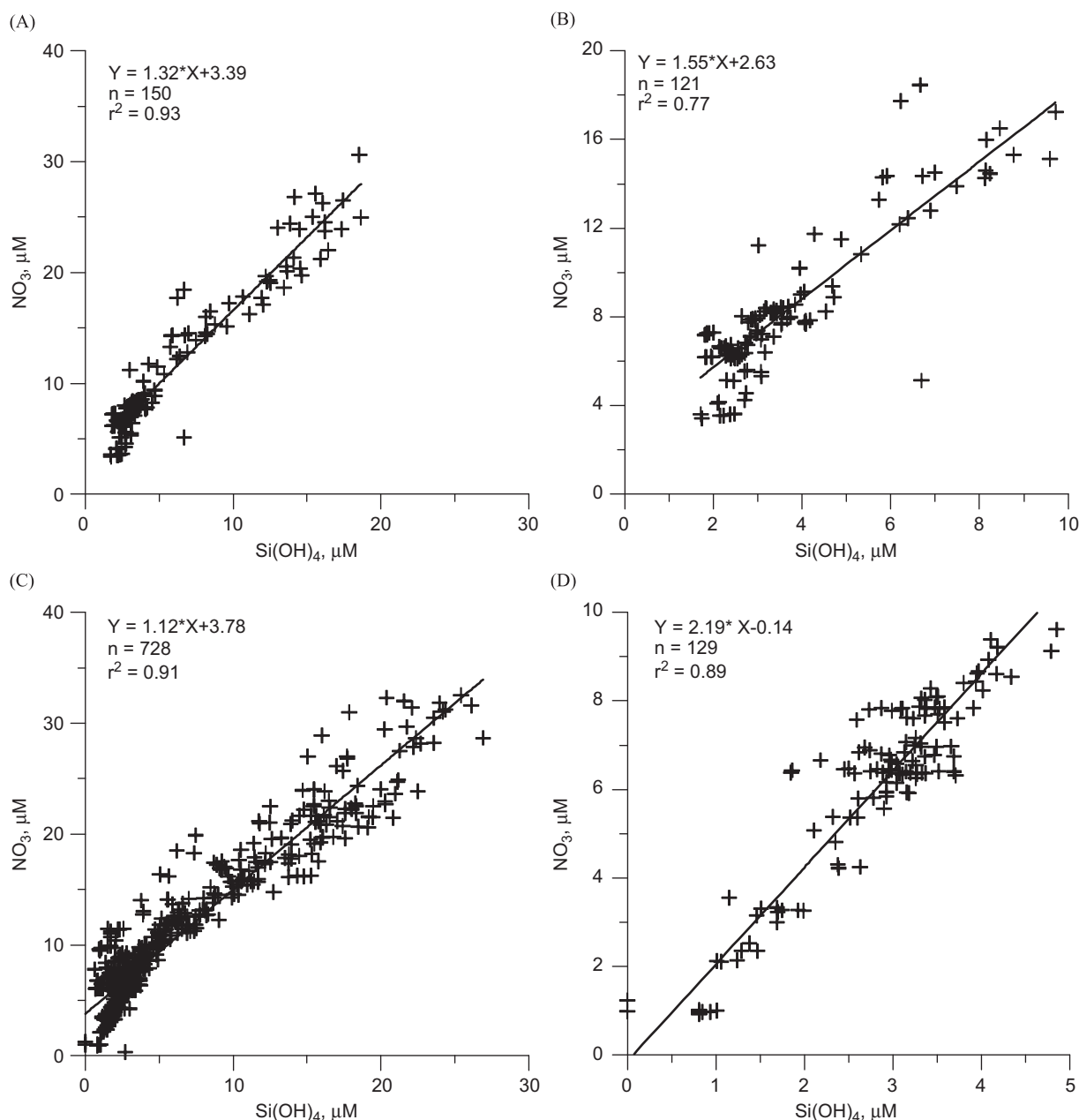
Fig. 2. NO_3 versus $Si(OH)_4$ concentrations from 1°N to 1°S for A) EB04 surface to 200 m depth, B) EB04 near-surface samples with $< 10 \mu M$ $Si(OH)_4$, C) EB05 surface to 200 m depth, D) EB05 near-surface samples with $< 5 \mu M$ $Si(OH)_4$.

activity relies on complete inhibition of diatom activity by the Ge addition. Brzezinski et al. (2011) showed that at $Si(OH)_4$ concentrations of 8.7 μM (a value that is above maximum concentrations in the EUZ) growth of the diatom *Thalassiosira weissflogii* was completely arrested at Ge concentrations of 1.0 μM, one-third of the concentration used in +Ge growouts in EB04 and EB05. No effect on growth of other non-siliceous phytoplankton was observed at concentrations up to 30 μM Ge. Incomplete inhibition of diatoms by Ge, unlikely in this case, will lead to an underestimate of actual diatom NO_3 drawdown so that the estimates of diatom NO_3 uptake are conservative. Diatom NO_3 uptake was equivalent to an average of 63% $\pm$ 16% (s.d.) of the total measured NO_3 drawdown during the nine experiments (Table 3). This percentage was then applied to the mean $\rho NO_3 T$ uptake measured during EB04 and EB05 (1°N - 1°S) using GF/F filters to capture uptake by all the phytoplankton; 7.10 and

8.34 nmol N L^{-1} h^{-1} to give the mean diatom fraction of the NO_3 uptake, 4.47 and 5.26 nmol N L^{-1} h^{-1} and > 5-μm non-diatom uptake rates of 1.09 and 0.53 nmol N L^{-1} h^{-1}. These values for mean NO_3 uptake attributable to diatoms using the +Ge estimate are close to the measured $^{15}NO_3$ uptake in the > 5-μm fraction, 5.56 on EB04 and 5.79 nmol N L^{-1} h^{-1} on EB05 (Table 2).

An indirect approach (Approach 4) uses measurements of mean $Si(OH)_4$ uptake ($\rho Si = 1.97$ and 1.79 nmol L^{-1} h^{-1} (Table 2) (Krause et al., 2011) multiplied by the diatom biomass ratio of Si:N measured by Baines et al. (2011) of 1:1 (also Brzezinski, 1985). This gives estimates of NO_3 uptake by diatoms of 1.97 and 1.79 nmol N L^{-1} h^{-1} for EB04 and EB05, respectively. This is only $\sim 25\%$ (21–28%) of the NO_3 uptake measured with ^{15}N for the > 5-μm size class and would indicate that non-diatoms in the > 5-μm size are taking up 3.59 and 4.0 nmol N L^{-1} h^{-1} or about 75% of > 5-μm NO_3 uptake (Table 2). Similarly, Approach 5 uses

Table 2
Measured equatorial NO_3 and $Si(OH)_4$ uptake (1°N to 1°S) and estimates of NO_3 uptake by diatoms and non diatoms > 5-μm in size. Values are the mean of upper 3 light levels (100%, 52%, 13%).

Approach		$\rho Si(OH)_4$	$\rho NO_3 T$	$\rho NO_3 < 5$-μm	$\rho NO_3 > 5$-μm	ρNO_3 diatoms	$\rho NO_3 > 5$-μm non diatom	% total ρNO_3 diatoms
		$nmol^{-1} h^{-1}$						
1. Measured values	EBO4	1.97	7.10	1.54	5.56	5.56	0	78.30
	EBO5	1.79	8.34	2.55	5.79	5.79	0	69.40
2. Using Parker et al. slope=0.87	EBO4					6.17	−0.61	87.00
	EBO5					7.26	−1.47	87.00
3. +Ge=63% of total ρNO_3	EBO4					4.47	1.09	63.00
	EBO5					5.26	0.53	63.00
4. Diatom Si:N biomass of 1:1	EBO4					1.97	3.59	27.76
	EBO5					1.79	4.00	21.43
5. $NO_3:Si(OH)_4$ slopes (Fig.2)	EBO4					3.05	2.50	43.03
	EBO5					3.92	1.87	46.94
6. Chemostat $\rho NO_3:\rho Si(OH)_4$	EBO4					6.23	−0.67	87.72
	EBO5					5.65	0.14	67.73
7. EBO5 $\rho NO_3 > 5$-μm:$\rho Si(OH)_4$	EBO5					6.26	-0.47	75.10

Table 3
Estimate of diatom contribution to NO_3 uptake from analysis of NO_3 drawdown in control vs. germanium addition treatments during 96-120-h experiments conducted during EB04 and EB05.

Cruise	Experiment	Treatment	NO_3, μM T_0	NO_3, μM T_{96} or T_{120}	ΔNO_3, μM drawdown	% of NO_3 uptake by diatoms
EB04	41	Control	3.61	1.26	2.35	
		+Ge	3.61	3.20	0.41	83%
	51	Control	7.78	4.20	3.58	
		+Ge	7.78	6.48	1.30	64%
	61	Control	6.03	2.58	3.45	
		+Ge	6.03	4.23	1.80	48%
	11	Control	6.1	3.14	2.96	
		+Ge	6.1	4.99	1.11	63%
	21	Control	8.27	3.40	4.87	
		+Ge	8.27	6.01	2.26	54%
	31	Control	7.38	5.26	2.12	
		+Ge	7.38	7.18	0.20	91%
EB05	12	Control	6.35	4.60	1.75	
		+Ge	6.35	5.68	0.67	62%
	22	Control	6.62	1.13	5.49	
		+Ge	6.62	4.60	2.02	63%
	32	Control	5.57	2.40	3.17	
		+Ge	5.57	3.66	1.91	40%
mean ± s.d.						63% ± 16%

Diatom NO_3 uptake was estimated as the difference between NO_3 drawdown observed in the control and NO_3 drawdown in the +Ge treatment at the end of the incubation (i.e. ΔNO_3cont - ΔNO_3Ge)/ΔNO_3cont). NO_3 concentrations at T0 and T96 (in EB05), T120 (in EB04) are the average of two bottle replicates.

the slopes of near surface concentrations of NO_3 versus $Si(OH)_4$ (Fig. 2B: slope=1.55, Fig. 2D: slope=2.19) to estimate the NO_3 uptake associated with $Si(OH)_4$, yielding values of 3.05 and 3.92 nmol N L^{-1} h^{-1}, 43-47% diatom NO_3 uptake. Comparing these estimates with the measured $\rho^{15}NO_3$ rates for the > 5-μm size fraction leaves 2.50 and 1.87 nmol N L^{-1} h^{-1} to be attributed to non-diatoms in that size fraction for EB04 and EB05, respectively

The ratios of NO_3T:$Si(OH)_4$ uptake in the EB04 (there were few fractionated measurements made on EB04) were plotted as a function of percent surface irradiance at which the water was sampled and incubated (Fig. 3). This shows the ratio changes with available irradiance (i.e. with depth) with ratios of nearly 4:1 with high irradiance in the bottles collected and incubated from the surface and 32% surface irradiance (32%LPD), then decreasing to nearly 1:1 at 5% surface irradiance followed by an increase to about 5:1 at the 0.8% light level. The decrease in the uptake ratio from high to low with decreasing irradiance (~depth) and an increase at the lowest irradiance is consistent with the pattern in

chemostat cultures of the diatom Skeletonema costatum held at decreasing irradiances (Davis, 1976), also plotted in Fig. 3. The agreement between the chemostat experiments and the EB04 data indicates that decreased irradiance with depth results in decreased $NO_3:Si(OH)_4$ uptake ratios for diatoms. For EB05, ratios of $NO_3:Si(OH)_4$ uptake are plotted for both NO_3 uptake by the > 5-μm cell-size fraction (Fig. 4A) and the total (GF/F) community (Fig. 4B) since size fractionation was done at most stations. The patterns of both fractions are similar and show the decrease with light followed by an increase at the lowest levels as in EB04 and the diatom chemostat data (Fig. 3). The ratio of $NO_3:Si(OH)_4$ uptake from the diatom chemostat of 3.16 was applied to the measured $Si(OH)_4$ uptake in Table 2 and resulted in estimates of diatom N uptake of 6.23 and 5.65 nmol N L^{-1} h^{-1} for EB04 and EB05 (Approach 6) The EB04 value was higher than the measured ρNO_3 for the > 5-μm size fraction by 0.67 nmol N L^{-1} h^{-1}. The EB05 value was within 2% of the ρNO_3 value measured for the > 5-μm size fraction, leaving only 0.14 nmol N L^{-1} h^{-1} as the estimate for non-diatom uptake. For EB05, the ratio of ρNO_3 in
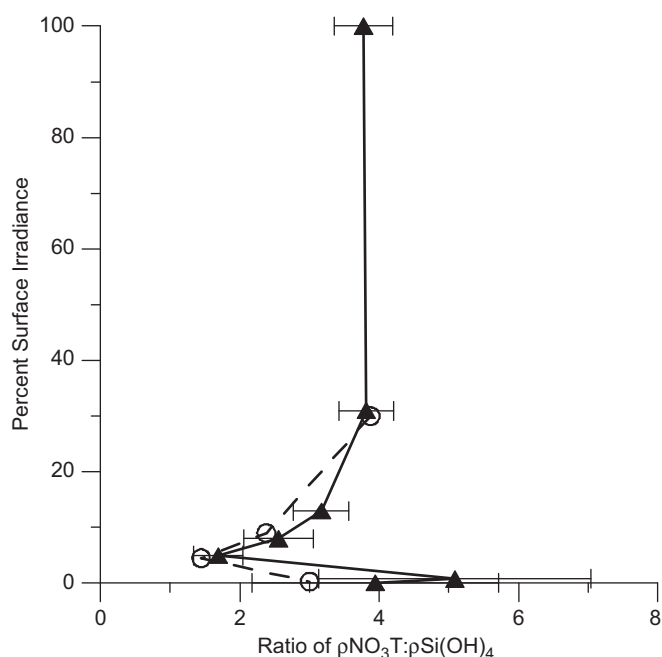
Fig. 3. Ratio of ρNO_3 by the total phytoplankton community to $\rho Si(OH)_4$ plotted as a function of percent surface irradiance (where collected and incubated) from EB04. Dotted line shows same pattern of $\rho NO_3 : \rho Si(OH)_4$ vs. irradiance in chemostat cultures of the diatom *Skeletonema costatum* (from Davis, 1976).

> 5-μm fraction:$\rho Si(OH)_4$ of 3.5 at the surface (Fig. 4A) was applied to the $Si(OH)_4$ uptake value (Table 2) and gave an estimate of diatom NO_3 uptake of 6.26 nmol N L^{-1} h^{-1} (Approach 7).

Using the 1:1 NO_3 to $Si(OH)_4$ uptake ratio, and the mean cruise $\rho Si(OH)_4$ values (Approach 4), yields the lowest estimates of the mean proportion of diatom to $\rho NO_3 T$ of 21 and 28% (Table 2), half of the next highest estimates. These low estimates may be inaccurate for two reasons. First, the X-Ray Fluorescence estimates (Baines et al., 2011) of Si:N cellular ratios are based on calculation of N from a proxy element (sulfur). Second, the reported ratio of N:Si of 1:1 is very much at odds with $Si(OH)_4$ limited chemostat measurements of cellular N:Si ratios, 3.16 (from Davis, 1976, see above). The first two approaches (Table 2) yield the highest values and over estimates of percentage of total NO_3 uptake by diatoms since they assume all calculated > 5-μm NO_3 uptake is by diatoms. The calculations (Approach 5) using the $NO_3 : Si(OH)_4$ slopes (Fig. 2) make the same assumption after assigning all calculated NO_3 uptake to the > 5-μm size class. These slopes may underestimate the uptake of either NO_3 or $Si(OH)_4$ or both due to *in situ* regeneration (Demarest et al., 2011). The agreement in uptake ratios as a function of irradiance between the chemostat and the irradiance profiles (Figs. 3 and 4) lend credence to the range of proportion of diatom uptake calculated by these approaches (Approach 6; 68 – 88% and Approach 7; 75%) (Table 2). These percentages, along with the +Ge estimate of 63% support the higher values (i.e. a range of 63 - 88%) as representative of conditions in the EUZ. Krause et al. (2011) reported estimates of a range of percent total NO_3 uptake by diatoms of 13 - 54%.

3.3. Partitioning NH_4 uptake between phytoplankton groups

To evaluate whether the picoplankton (classified here as < 5-μm sized cells) are the major users of NH_4 as proposed by Dugdale and Wilkerson (1998), size-fractionated $^{15}NH_4$ uptake measurements were made during EB04 and EB05. Upper water column values (52% for EB04 and 52% and 31% for EB05) are given
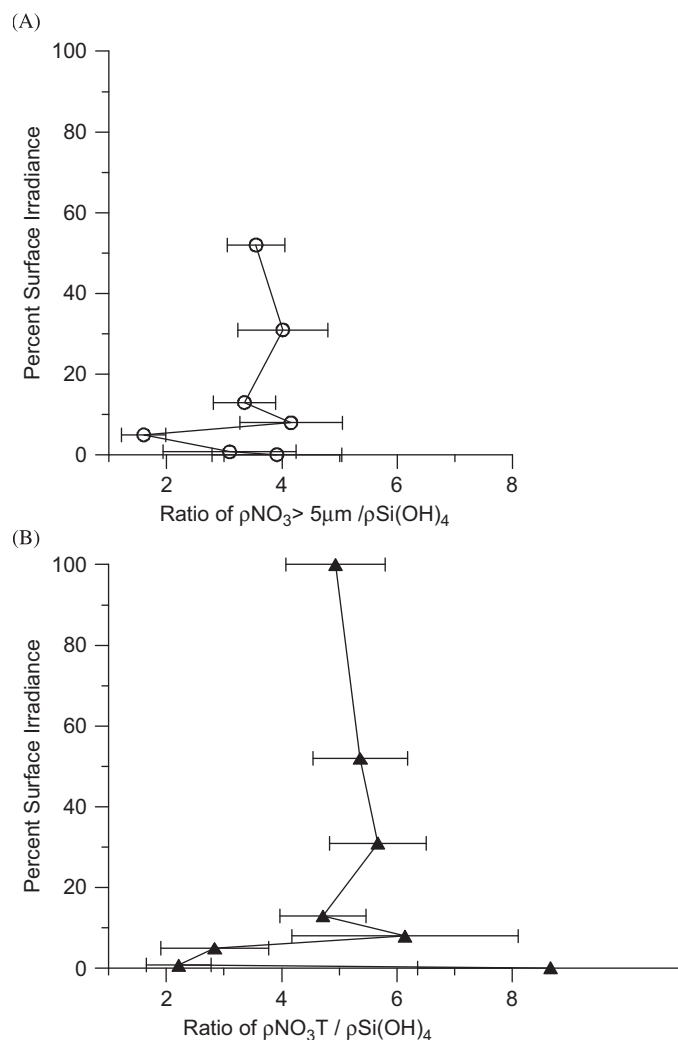

Fig. 4. A) Ratio of ρNO_3 by cells > 5-μm to $\rho Si(OH)_4$ and B) ratio of ρNO_3 by the total phytoplankton community to $\rho Si(OH)_4$ plotted as a function of percent surface irradiance (where collected and incubated) from EB05.

Table 4
Size-fractionated NH_4 uptake and f-ratio measured between 1°N to 1°S (mean of upper 3 light levels, 100%, 52% and 13%).

	ρNH_4 nmol L^{-1} h^{-1}		
	all cells	< 5-μm cells	> 5-μm cells
EB04	8.57	4.78	3.79
EB05	17.75	11.25	6.50
	f-ratio		
	all cells	< 5-μm cells	> 5-μm cells
EB04	0.45	0.24	0.59
EB05	0.32	0.19	0.47

in Table 4. More than half of the NH_4 uptake is carried out by the smaller cells (< 5-μm size class) 4.78 nmol N L^{-1} h^{-1} (56% in EB04) and 11.25 nmol N L^{-1} h^{-1} (63% in EB05). The f-ratios (i.e. $\rho NO_3 / \rho NO_3 + \rho NH_4$) for the different size fractions (picoplankton < 5-μm; and cells > 5-μm) were calculated for EB05, based on measured rates (Table 2). The mean f-ratios for the picoplankton, 0.24 and 0.19, are about twice that predicted in Dugdale and Wilkerson (1998) of 0.1 and by the CoSiNE (Chai et al., 2002)

model (0.16), and consistent with a primarily regenerated production picoplankton community using some NO_3, but mostly NH_4. The measured fractionated $^{15}NH_4$ and $^{15}NO_3$ uptake rates yield an f-ratio of 0.59 (EB04) and 0.47 (EB05) for the $> 5\text{-}\mu m$ fraction, in good agreement with CoSiNE model of f-ratio$=0.6$ for a large range of source $Si(OH)_4$ concentrations.

3.4. Silicate and nitrate uptake kinetics from station data (collected at 52% LPD)

Details of the $Si(OH)_4$ uptake versus $Si(OH)_4$ concentration kinetics measurements are given in Brzezinski et al. (2008, their Table 1). The data have been condensed and reproduced here (Table 5) so that these equatorial field results can be compared with uptake kinetics obtained from chemostat cultures of diatoms under $Si(OH)_4$ limitation (Dugdale et al., 1981). During EB04 and EB05, phytoplankton in water collected from 52% LPD and incubated at 50% surface irradiance showed increased $Si(OH)_4$ uptake in response to a series of increased $Si(OH)_4$ concentrations (up to 15 μM $Si(OH)_4$ above ambient), as reflected by V'_{maxSi} values (biomass specific uptake rate) greater than V'_{Si} measured at ambient $Si(OH)_4$. We use V'_{maxSi} rather than V_{maxSi} (Brzezinski et al., 2008) to indicate its variable nature and statistical derivation. V'_{Si} is equivalent to V_{Siamb} used by Brzezinski et al. (2008) and may be underestimated if detrital Si is present (see below). V'_{maxSi} is derived by fitting data points to the Michaelis-Menten equation from a series of incubations with added $Si(OH)_4$ and V'_{Si} is the uptake measured at the ambient concentration of $Si(OH)_4$. The mean V'_{Si} was slightly higher in EB04, $0.020\,h^{-1}$, than in EB05, $0.014\,h^{-1}$ with a mean of $0.017\,h^{-1}$. The mean V'_{maxSi} was also higher in EB04, $0.031\,h^{-1}$, than in EB05, $0.023\,h^{-1}$. The mean ratios of V'_{maxSi}/V'_{Si} were virtually identical in both EB04 and EB05, 1.64 and 1.67, respectively. The K'_{Si} values (the $Si(OH)_4$ concentration at which uptake is reduced to 1/2 V'_{maxSi}) for the two cruises, 1.70 and 1.55 μM, are statistically the same with an overall mean of 1.63 μM. The overall mean V'_{maxSi} was $0.026\,h^{-1}$. These values are somewhat lower than the only previously published values for the equatorial Pacific, $K'_{Si}=2.42$ μM and $V'_{maxSi}=0.052\,h^{-1}$ (Leynaert et al., 2001) and for the values used in the CoSiNE one dimensional model (Chai et al., 2002), $K'_{Si}=3.0$ μM and $V'_{maxSi}=0.062\,h^{-1}$.

To observe changes in NO_3 uptake with increasing NO_3 concentrations, water collected from the 52% LPD during EB04 was incubated at 50% surface irradiance with either $^{15}NO_3$ enrichment, at 10% of ambient NO_3 (termed trace) or with 5 μM $^{15}NO_3$ additions (termed saturated) (Table 6). The ambient NO_3 concentrations were about 6 μM at all the stations in Table 6 (Dugdale et al. 2007), well above typical reported K'_{NO3} values of about 2 μM. No consistent response to added NO_3 was observed (Table 6), i.e. uptake with 5 μM NO_3 addition was the same as with 10% of ambient NO_3 concentration, with a mean ratio of $V_{trace}:V_{sat}$ of 0.98. The mean trace V_{NO3}, $0.012\,h^{-1}$ is the same as the mean V_{NO3sat}. The stations sampled overlapped with but were not exactly the same stations as those sampled for $Si(OH)_4$ kinetics by Brzezinski et al. (2008).

3.5. Delayed silicate and nitrate uptake kinetics from enclosures/grow outs

During EB05, $Si(OH)_4$ and NO_3 uptake kinetics were measured in a series of shipboard on-deck carboy/enclosure experiments using equatorial water collected using the trace-metal clean rosette system (TM-rosette) from mid euphotic zone depths (15 - 30 m, approx. 13 - 30% LPD) and incubated at 50% of surface irradiance. $Si(OH)_4$ and NO_3 uptake versus substrate concentrations were measured during two experiments (one control and one with added Fe) when the carboys were first filled (i.e. time zero), and then after 24, 48 and 96 hours. These experiments were replicated at four stations. Little changes in kinetic variables occurred in the enclosures during the first 24 hours (Brzezinski et al., 2008), and the most meaningful kinetic data in response to the treatments was obtained after a delay of 48 or 96 hours. The 48 hour values are the most useful since little change in population size occurred by that time. To be able to use perturbations in on-deck experiments to understand processes occurring in the water column, there needs to be good agreement between on-deck baseline data and in situ conditions. The mean values obtained for the EB05 stations where $V'_{maxSi}=0.023 \pm 0.005\,h^{-1}$, $K'_{Si}=1.55 \pm 0.59\,\mu M$ (Table 5) and $V'_{maxNO3}=0.012$ h^{-1} (Table 6, K'_{NO3} not measureable due to lack of response to added NO_3) can be used as baseline in situ conditions to compare with on-deck enclosures at time zero; $V'_{maxSi}=0.015\,h^{-1}$, $K'_{Si}=1.62 \pm 1.14\,\mu M$ (Brzezinski et al., 2008) and the range of V'_{maxNO3} of 0.016 - 0.032 h^{-1} (Table 7) and show the on-deck data is well constrained, with lack of significant differences between the nutrient uptake kinetics measured using water from stations and on-deck enclosures at time zero.

Table 6
NO_3 uptake measured during EB05 using ambient NO_3 concentration (trace) and with added NO_3 concentrations (5 μM, saturated).

Station	VNO_3, h^{-1} trace	VNO_3, h^{-1} saturated	trace:saturated
2	0.004	0.009	0.43
3	0.010	0.010	1.00
4	0.012	0.009	1.28
5	0.008	0.011	0.67
7	0.013	0.015	0.90
9	0.013	0.007	1.89
10	0.008	0.008	0.95
11	0.006	0.004	1.46
12	0.005	0.007	0.64
14	0.014	0.015	0.92
16	0.011	0.010	1.11
18	0.001	0.003	0.19
20	0.025	0.020	1.26
22	0.012	0.012	1.05
24	0.012		
26	0.023	0.021	1.07
28	0.016	0.017	0.94
29	0.018	0.020	0.91
mean	0.012	0.012	0.98
s.d.	0.006	0.005	0.39

Table 5
$Si(OH)_4$ uptake kinetic data (mean $\pm$ s.d) from EB04 and EB05 station samples incubated at 50% surface irradiance.

	V'_{maxSi}, h^{-1}	V'_{Si}, h^{-1}	$V'_{maxSi}:V'_{Si}$	K'_s, μM	Fe, nM	$Si(OH)_4$, μM	Fe, nM
EB04 (n=15)	0.031 ± 0.007	0.020 ± 0.006	1.64	1.70 ± 0.95	0.16 ± 0.12	2.86 ± 0.87	0.16 ± 0.12
EB05 (n=14)	0.023 ± 0.005	0.014 ± 0.003	1.67	1.55 ± 0.59	0.33 ± 0.2	2.46 ± 0.65	0.33 ± 0.20
EB04 +EB05	0.026 ± 0.007	0.017 ± 0.006	1.66	1.63 ± 0.79	0.24 ± 0.18	2.66 ± 0.78	0.24 ± 0.18

$V'_{maxSi}:V'_{Si}$ is equivalent to $V_{Si}:V_{amb}$ of Brzezinski et al. (2008).

Table 7
Si(OH)$_4$ and NO$_3$ uptake kinetics measured in experimental on-deck enclosures 0, 48 and 96 hours after filling with upper euphotic zone water during EB05 (controls) or amended with 2 nM Fe (+Fe).

Cast	Elapsed Time, h	Ambient Concentration		Control			+Fe		
		Fe, nM	Si(OH)$_4$, µM	K'$_{Si}$ µM	V'$_{maxSi}$, h^{-1}	V'$_{maxNO3}$, h^{-1}	K'$_{Si}$ µM	V'$_{maxSi}$, h^{-1}	V'$_{maxNO3}$, h^{-1}
7.06	0	0.23	2.61			0.016			0.017
	48			1.80	0.060	0.128	3.52	0.083	0.071
	96								0.089
13.06	0	0.56	2.95			0.032			0.020
	48			3.08	0.059		1.12	0.087	
	96					0.054			0.075
19.05	0	0.11	3.38			0.022			0.022
	48		2.70	2.48	0.044		0.68	0.060	
	96					0.077			0.068
22.05	0	0.09							0.023
	48			0.83	0.031		1.07	0.076	
	96					0.073			
mean				2.05	0.049		1.6	0.077	0.077*
sd				0.97	0.01		1.3	0.010	0.030

Mean values are from 48-h data except for * when mean calculated from 96-h data.

Compared to station data, the greatest response shown by V'$_{maxSi}$ was after the water was enclosed and held on deck for 48 h, a 113% increase (V'$_{maxSi}$ increase between ambient station data, 0.023 h^{-1} and the controls-Table 7, 0.049 h^{-1}). An additional 58% increase in V'$_{maxSi}$ occurred with the addition of Fe to the enclosures (0.077 h^{-1}, Table 7). The V'$_{maxNO3}$ values in the controls after 96 h were 0.054 and 0.77 h^{-1}. An increase in V'$_{maxNO3}$ occurred with the addition of Fe in one experiment to 0.075 h^{-1} but decreased in the other to 0.068 h^{-1}, respectively (Table 7). The mean values of V'$_{maxSi}$ and V'$_{maxNO3}$ with added Fe were the same at the longer incubation times, 0.077 h^{-1} respectively (but note the differences in sampling times, 96 and 48 hours used to calculate the means). The specific uptake rates obtained in all these tracer uptake measurements are subject to dilution effects from the presence of detrital particulate material; the values of V'$_{Si}$ and V'$_{NO3}$ reported here should be considered to be relative rather than absolute. During EB04 and EB05, the detrital Si was estimated to be 68% of the total BSi by Brzezinski et al. (2008).

3.6. Interpretation of nutrient uptake kinetics using chemostat kinetics

3.6.1. Chemostat kinetics

Following the Frost and Franzen (1992) analysis of the EUZ as a chemostat, we used that approach here to interpret the Si(OH)$_4$ and NO$_3$ uptake and kinetic data. The kinetics of uptake of the limiting nutrient was studied in chemostat cultures of the diatom *Skeletonema costatum* by Conway et al. (1976) using chemostats with NH$_4$ limitation, by Harrison et al. (1976) with Si(OH)$_4$ limitation and by Davis (1976) to examine the interaction of light effects with Si(OH)$_4$ limitation. The results of those studies, synthesized by Dugdale et al. (1981), provide a basis for analyzing the EB04 and EB05 station and delayed kinetics data and understanding the functioning of the Si(OH)$_4$-limited equatorial diatom production system. The uptake kinetics that occur with one limiting nutrient and those that result when there is interaction of the limiting nutrient control with other potential limiting factors are first reviewed and then the EB04 and EB05 uptake kinetics data are compared with results from laboratory diatom chemostats and the CoSiNE model.

Chemostats are simple devices consisting of a reactor (vessel) containing cells (here, diatoms) and a nutrient medium made up to assure one nutrient will be in limiting supply relative to the needs of the organism being grown. A pump supplies the medium to the reactor and the medium and organisms exit the reactor at the pumping rate, leaving some cells in the reactor. The ratio of pumping rate (F) to volume of the reactor (V) is termed the dilution rate (D), and this sets the loss rate of nutrient medium and organisms. At steady state, the growth rate (μ) of the cells equals the loss rate:

$$\mu = D = F/V, \text{units of } t^{-1} \tag{2}$$

To attain and maintain steady state, negative feedback between the limiting nutrient concentration and limiting nutrient uptake rate must exist. In Si(OH)$_4$-limited diatom chemostats Dugdale et al. (1981) showed this stabilizing feedback to be provided through Michaelis-Menten kinetics, according to:

$$V_{Si} = V'_{maxSi}*[Si(OH)_4]/(K'_{Si}+[Si(OH)_4]) \tag{3}$$

where V$_{Si}$ is the biomass-specific uptake rate of Si(OH)$_4$, V'$_{maxSi}$ is the maximal biomass-specific uptake rate of the cultured diatom with saturating Si(OH)$_4$ concentration. The value of V'$_{maxSi}$ depends upon the environmental conditions provided (e.g. temperature, irradiance, etc), and K_{Si} is the Si(OH)$_4$ concentration at which V$_{Si}$=V'$_{maxSi}$/2.

These relationships between limiting nutrient concentration, limiting nutrient uptake rate and dilution rate in a chemostat are illustrated in Fig. 5, using Si(OH)$_4$ as the limiting nutrient. Eq. (3) is used to plot the Michaelis-Menten hyperbolic relationship. At steady state, the growth rate (μ) is set by the loss rate, D (Eq. (2)) (or grazing in the equatorial system) shown arbitrarily on the Y-axis at the operating V$_{Si}$ (at 0.0425 h^{-1} in Fig. 5). The operating (ambient) concentration of the limiting nutrient in the reactor is set by the intersection of D with the Michaelis-Menten hyperbola for uptake of the limiting nutrient (Si(OH)$_4$ and projected to the X-axis (the concentration of limiting nutrient) (Fig. 5). If due to some perturbation Si(OH)$_4$ concentration rises above that required for the steady-state growth rate (i.e. 2 µM in Fig. 5), excess uptake occurs, reducing the ambient Si(OH)$_4$ concentration back toward the steady-state value and providing the necessary negative feedback value for stability.

At steady state, the growth rate μ, and all biomass-specific uptake rates (V) must be the same, and equal to the dilution rate with units t^{-1}

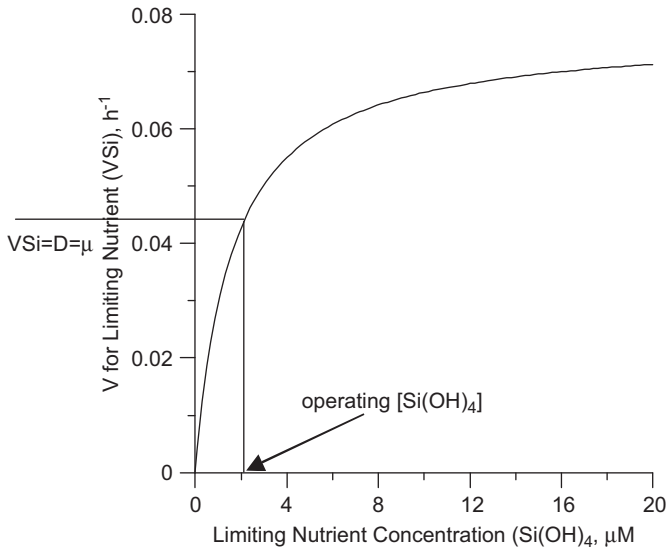$$\mu = D = V_{Si} = V_N = Vc \ldots \ldots \text{etc} \tag{4}$$

Fig. 5. Michaelis-Menten hyperbola showing the specific uptake rate of a limiting nutrient (here, V_{Si} set by the dilution rate $D = \mu$) vs. the limiting nutrient concentration (here, $Si(OH)_4$ concentration). Arrow on the X axis shows the operating $Si(OH)_4$ concentration required to maintain the set growth rate (Eqn. 2).

Table 8
Mean uptake rates during two $Si(OH)_4$ limited perturbation experiments with *Skeletenoma costatum* chemostats (from Davis, 1976) with dilution rate, $D = 0.04\ h^{-1}$.

Dilution rate	V'_{PO4}, h^{-1}	V'_{NO3}, h^{-1}	V'_{maxSi}, h^{-1}	V'_{maxSi}:V'_{NO3}
0.040	0.040	0.04	0.07	1.75
0.041	0.038	0.04	0.06	1.50
mean				1.60

which is equivalent to:

$$\mu = \rho Si / BSi = \rho N / PON = \rho C / POC \ldots \ldots \text{etc} \qquad (5)$$

The *V*'s for the non-limiting nutrients (in Eqn 4 these would be V_N and V_C) are fixed in the sense that they do not vary in response to changes in their substrate, as required by Eqn. 4. For the negative feedback necessary to stabilize the chemostat culture, uptake of limiting nutrient (V_{Si} in Fig. 5), Eqn. 3, must be allowed to vary with limiting substrate concentration (i.e. a Michaelis-Menten response), with a maximal value of V'_{maxSi} that must be greater than the operating V_{Si} ($= D = \mu$). In $Si(OH)_4$ limited chemostats of the diatom *S. costatum*, Davis (1976) used dilution rates D of 0.040 and 0.041 h^{-1} and showed that $V'_{max\ Si}$, was about 1.6 times the operating V (Table 8). The values of $V'_{max\ Si}$, 0.07 h^{-1} and 0.06 h^{-1} are well above D (0.04 h^{-1}) while those for V_{NO3} (0.04 h^{-1}) and V_{PO4} (0.04 h^{-1}) are equal to the dilution rate (Table 8) as required for steady state by Eqn. 4.

V'_{maxSi} may be reduced if some other environmental factor becomes limiting, i.e. sets the maximum growth rate that can be achieved under those specific environmental conditions. Davis (1976) showed that in the *S. costatum* chemostats, the value of V'_{maxSi} was a function of the irradiance provided.

$$V'_{maxSi} = V_{maxSi} * I / (K_I + I) \qquad (6)$$

where V_{maxSi} is the maximal rate at saturated irradiance, I=mean irradiance, K_I is the irradiance at which V'_{maxSi} is reduced to $\frac{1}{2}V_{maxSi}$. In the Davis (1976) experiments, $K_I = 0.07$ ly min^{-1}, $V_{maxSi} = 0.12\ h^{-1}$. If the V'_{max-Si} decreases and approaches or

equals the operating V_{Si}, the system will become unstable and the culture washes out (Dugdale, 1967; Dugdale et al., 2007), for example by reduced light.

The results from the station data collected during EB04 and EB05 (Table 5) show that the equatorial Pacific likely is functioning as a diatom $Si(OH)_4$-limited system with a mean V'_{Si} of about 0.017 h^{-1} and a mean V'_{maxSi} of 0.026 h^{-1}. These rates are well above dilution rates (0.0004 h^{-1}=0.01 d^{-1}) calculated for the equatorial euphotic zone (chemostat volume) of 100 m and a nutrient supply rate (upwelling rate) of 1 m d^{-1}. The calculated values are low in comparison with the overall loss rates that are dominated by grazing. The ratio of V'_{maxSi}/V_{Si} of 1.66 in this data set is nearly the same as in the chemostat experiments of Davis (1976), 1.6 (Table 8) confirming that $Si(OH)_4$ regulation of $Si(OH)_4$ uptake and growth could be achieved in the equatorial system since by analogy, the chemostat diatom population maintained steady state with this range of kinetics. The question remains: what environmental variable sets the value of V'_{maxSi} in the equatorial ecosystem? Two likely candidates are: 1) mean irradiance (Davis 1976) and 2) euphotic zone Fe (Brzezinski et al., 2008). The chemostat diatom studies of Davis (1976) and the culture studies of the effect of Fe on diatom $Si(OH)_4$ uptake kinetics (Leynaert et al., 2004) will be used to interpret the variations in V'_{maxSi} in both station and on-deck enclosure data during EB05.

3.6.2. Effect of irradiance

Large increases occurred in V'_{maxSi} and in V'_{maxNO3} (Table 7) with elapsed time in both control and +Fe enclosures. The control V'_{maxSi} (mean=0.049 h^{-1}) was greater than V'_{maxSi} measured in ambient conditions at stations (mean V'_{maxSi}=0.023, Table 5). The increase in mean V'_{maxSi} between ambient water (station data) and on-deck enclosures was actually greater (113% increase) than between control and added Fe treatments (55% increase from 0.049 to 0.077 h^{-1}). The increase in V'_{maxSi} and V'_{maxNO3} in the control enclosures is linked to taking the water and holding it on-deck; it could be due to the improved irradiance conditions as no other manipulations were made, although ambient physics changed and grazing pressure may change when water is enclosed and held on-deck. Measured uptake vs. irradiance kinetics made by Parker et al. (2011) show the K_I (the light intensity where NO_3 transport is reduced to half maximal) for NO_3 uptake to be 11.3 - 21% of surface irradiance. This indicates that phytoplankton moved from irradiances (depths) from below the K_I and incubated at irradiances above the K_I will show an increase in uptake according to Michaelis-Menten kinetics. Changes in the light regime occurred in these on-deck enclosures compared to the sampling depths as a result of the water capturing technique used to minimize contamination by Fe from the trace-metal clean rosette. The rosette was first lowered to 100 m, then raised slowly tripping bottles without stopping the winch, beginning ~13% LPD and ending ~30% LPD. The corresponding depths at 140°W, 0° were 30 m (13% LPD) and 15 m (30% LPD) respectively. Consequently there is no way to know precisely the ambient light regime experienced by these mixed samples that were used to fill the on-deck enclosures that were then incubated at 50% LPD. However, the possible effect of this change in irradiance on $Si(OH)_4$ uptake can be estimated since Krause et al. (2011, Fig. 8) found a linear relationship between the slope of the specific $Si(OH)_4$ uptake to ambient $Si(OH)_4$ concentration when plotted versus irradiance:

$$\text{Slope (of } V_{Si} \text{ vs. } Si(OH)_4) = 0.052 \times I + 0.36 \qquad (7)$$

Assuming no change in ambient $Si(OH)_4$ the calculated V_{Si} at 15 m depth (~30% LPD) is 65% of the calculated V_{Si} at the

enclosure irradiance (50% I_0), i.e. an increase of ~55% would be expected if 30% LPD water were brought to the surface and incubated on-deck at 50% I_0. The calculated change in V_{Si} between water sampled at 30 m depth (13% LPD) is only 35% of the calculated V_{Si} at the on-deck enclosure irradiance, i.e. an increase of ~185% would be expected if 13% LPD water were brought to the surface and incubated at 50% I_0. From these rough calculations, a major cause of increased Si(OH)$_4$ uptake rates in the control enclosures (113%, Section 3.5) can be attributed to the change in the irradiance field experienced in the on-deck enclosures. De Baar et al. (2005) analyzed all the available open ocean Fe enrichment experiments that had been conducted and concluded that the depth of the mixed layer, i.e. the light regime, and not Fe was the major factor determining the yield in phytoplankton biomass. On-deck enclosures done in parallel with *in situ* Fe fertilizations always resulted in increases in chlorophyll concentration in the on-deck controls (as occurred also in the EB04 and EB05 experiments), and the conclusion was reached that light was a more important factor than Fe in explaining the outcome of these fertilization experiments (De Baar et al., 2005). The one-dimensional physical-biological modeling work also supported the light regulation on the increase of phytoplankton biomass after Fe enrichment (Fujii and Chai, 2009).

3.6.3. Effect of Fe

The +Fe ondeck enclosures (carboys) showed increases over the control carboys, to a mean $V'_{maxSi} = 0.077$ h^{-1} (Table 7). However, the V'_{maxSi} values in the controls varied among the grow-out experiments (on-deck enclosures) and were always greater than in the station kinetics. The seawater used to fill the four experimental enclosures used for delayed kinetics in EB05 had a range of ambient Fe from 0.09 to 0.56 nM (Table 7) suggesting possible Fe modulation of Si(OH)$_4$ uptake. The range in ambient Fe concentrations in the control grow-outs (incubated with 50% surface irradiance) provides a way to examine the possible effects of Fe on V'_{maxSi} by assuming that low irradiance or some other unknown limitation was eliminated in the carboys held on-deck, leaving Fe as the next factor limiting V'_{maxSi}. Leynaert et al. (2004) studied the effect of Fe deficiency on Si(OH)$_4$ uptake kinetics of the diatom *Cylindrotheca fusiformis* using clean techniques to avoid Fe contamination at low concentrations. Both K'_{Si} and V'_{maxSi} varied with Fe concentrations, and the relationship was described by a Michaelis-Menten function of V'_{maxSi} versus Fe concentration, with a K'_{Fe} of 0.049 nM and a $V'_{maxSi} = 0.081$ h^{-1} (Leynaert et al., 2004).

$$V'_{maxSi} = V_{maxSi} * [Fe]/([K'_{Fe} + [Fe]) \qquad (8)$$

where V_{maxSi} is the maximum Si(OH)$_4$ uptake rate with saturating Fe under a given set of environmental conditions. K'_{Fe} is the concentration of Fe at which V'_{maxSi} is reduced to ½V_{maxSi}.

Making the assumption that the V'_{maxSi} in the EB05 control enclosures would be a function of Fe concentration (as in Leynaert et al., 2004), a Michaelis-Menten hyperbola was fitted to V'_{maxSi} from the delayed kinetics of the controls and ambient Fe from the enclosures of EB05, with an S/V vs. S linear plot (Walter, 1965) yielding a K_{Fe} of 0.086 nM and mean V'_{maxSi} of 0.069 h^{-1}. The resulting hyperbola was plotted along with the four control values for V'_{maxSi} (after 48 hrs elapsed time) versus Fe concentration (from Table 7) (Fig. 6) and suggests that with irradiance (or some other favorable) conditions in the surface ocean equivalent to those that occur in the control enclosures, variations in Fe concentration could influence the value of V'_{maxSi}. The Leynaert et al. (2004) hyperbola is also plotted in Fig. 6 for comparison with the EB05 results. The tendency of V'_{maxSi} to be a function of ambient Fe in the equatorial Pacific data appears quantitatively and qualitatively similar to the laboratory results of Leynaert et al.
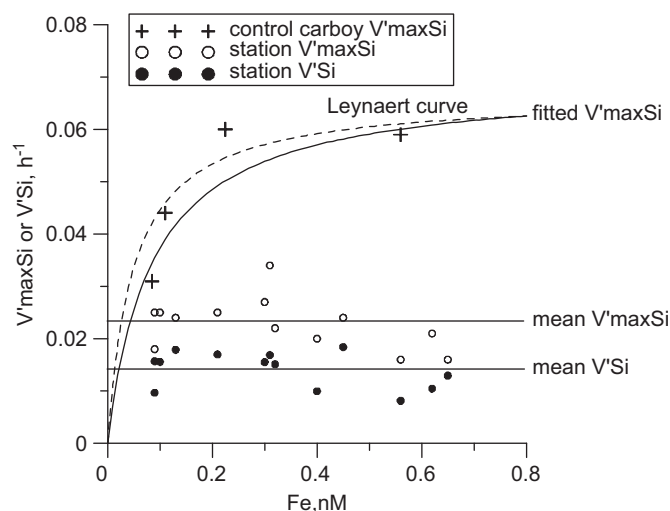

Fig. 6. Michaelis-Menten hyperbolic plot of V'_{maxSi} vs. ambient Fe concentration, as suggested by Leynaert et al. (2004). The + symbols are the values of V'_{maxSi} in the control carboys plotted against ambient Fe held on deck with 50% surface irradiance for 48 hours on EB05 (delayed kinetic experiments). The hyperbola marked "fitted V_{maxSi}" is plotted from a fit of the 4 data points. The hyperbola marked "Leynaert" is plotted from Leynaert et al. (2004) using $K_{Fe} = 0.049$ nM. The open circles are the V'_{maxSi} values for the kinetic experiments made on the 52% LPD samples at stations along the equatorial transect; the upper horizontal line is the mean of these station V'_{maxSi} values. The closed circles are the measured ambient (un-enriched) V'_{Si} rates. The lower horizontal line is the mean value of station V'_{Si} values. Data source: Brzezinski et al. (2008).

(2004). When the V'_{maxSi} values from the EB05 station data (i.e. without holding water in an on-deck enclosure) are plotted against ambient Fe concentration (Fig. 6), no variation in V'_{maxSi} with Fe is apparent and the values vary about the mean V'_{maxSi} for EB05 shown as the upper horizontal straight line. Some environmental variable other than Fe determines the maximum uptake of Si(OH)$_4$ in the station data. This is likely to be the mean irradiance since the value of V'_{maxSi} increased in all of the controls by 48 hours after enclosing the water and holding at 50% surface irradiance. Finally, the values of V'_{Si} (i.e. uptake at ambient Si(OH)$_4$ concentration) for the stations are plotted against Fe in Fig. 6 and fall along the line representing the mean V'_{Si}, below the line of V'_{maxSi} since the ratio of V'_{maxSi}:V_{Si} was 1.6 (Brzezinski et al., 2008 and Table 5). Neither V'_{maxSi} nor V'_{Si} show any relationship with ambient surface Fe concentration. This might be expected since all the initial Fe values in water samples where upwelling is in progress, except possibly at 110°W, are well above the K_{Fe} values of 0.086 nM (for V'_{maxSi}, an Fe-based half-saturation constant for Si(OH)$_4$ uptake).

3.6.4. Effect of Si(OH)$_4$

Measured specific Si(OH)$_4$ uptake, V'_{Si}, (station values) at the three upper sampling depths (from 100, 52, and 31% LPD) are plotted against ambient Si(OH)$_4$ concentration in Fig. 7 along with the uptake kinetics from two stations (one in EB05 and the other in EB04) representing the minimum and maximum hyperbolae obtained by Brzezinski et al. (2008, their Table 1). The data points would not be expected to fall along a single hyperbolic curve since the kinetics vary along the equator and consequently, each data point may be on a different hyperbola but within the range of kinetics, i.e. between the two curves in Fig. 7. The box outlined by dotted lines gives the range (but not the absolute values) of surface Si(OH)$_4$ concentrations and V'_{Si} for the diatoms predicted by the CoSiNE model for the range of source Si(OH)$_4$ concentrations (i.e. from 120m depth) experienced in the eastern equatorial

Pacific. The data from EB05 mostly fit in the box predicted by the model.

3.6.5. Cascade of limitations on V'_{maxSi}

A pattern of regulatory mechanisms of the equatorial quasi-chemostat system similar to that described for diatom chemostat cultures emerges from the data analysis of uptake kinetics measured at stations and in shipboard experimental enclosures (Fig. 8). First, the chemostat study of Davis (1976), showed that irradiance could set the V'_{maxSi} and the growth rate μ'_{max} of a diatom chemostat culture (Fig. 8, left panel). An irradiance regulation of V'_{maxSi} could set the maximal $Si(OH)_4$ uptake kinetics (upper red dotted line, central panel), e.g. as measured in shipboard enclosures during EB05. The mean measured V'_{Si}
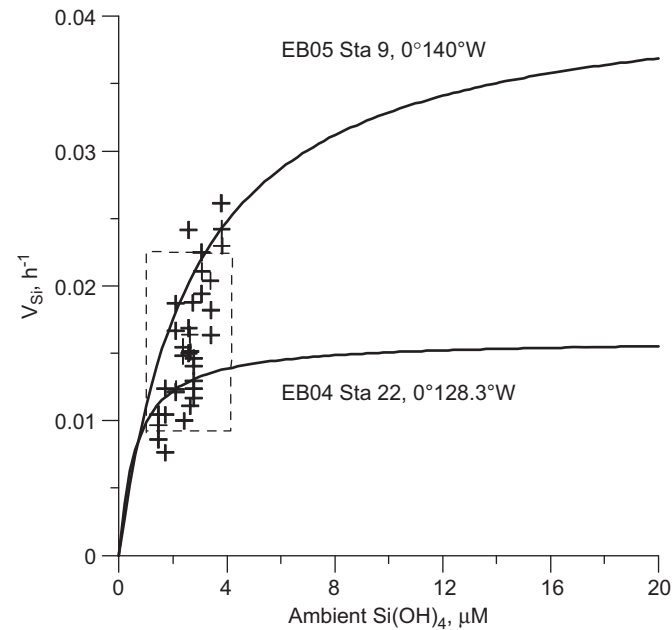
Fig. 7. Minimum and maximum kinetic curves from Brzezinski et al. (2008) with crosses showing V_{Si} measured during EB05 from 1°N to 1°S (samples from upper LPD's). Box is the predicted V_{Si} and $Si(OH)_4$ data from the CoSiNE model (see text).

(lower black dotted line in central panel) is shown as the operating V'_{Si} labeled V_L (loss rate) equivalent to D in a chemostat but here due mainly to grazing. The operating V'_{Si} is projected down from the intersection with the $Si(OH)_4$ uptake hyperbola to the X axis (vertical black dotted line) to denote the ambient $Si(OH)_4$ concentration required to support the loss rate. This rate, V'_{Si} will also equal the V'_{max} of the non-limiting nutrient (Eqn. 3, Table 8). In EB05, this would be V'_{maxNO3}. In this scheme, the growth-limiting factor that is setting V'_{maxSi} ($=\mu'_{max}$) is assumed to be irradiance and $Si(OH)_4$ the limiting nutrient. In nature, the mean irradiance will have some variability. Consequently the operating point (ambient $Si(OH)_4$ concentration) will vary even if the loss rate remains constant.

The results of the enclosure kinetics, enclosure delayed kinetics, station kinetics and station (ambient) $Si(OH)_4$ uptake rates are summarized as a downward cascade of limitations on V_{max} or μ_{max} in Fig. 9. Each of the steps from one limitation to the next is illustrated by data (Tables 5, 7). The organism (diatom) V_{max} is estimated (0.077 h^{-1}) from the delayed kinetics (Table 7 and Brzezinski et al., 2008) with both Si and Fe additions. When only Fe is added the delayed kinetics are reduced to the line marked "V'_{maxSi} with added Fe". With no additions to the water, but manipulating the water by enclosure on-deck, V'_{maxSi} is reduced to the line marked "Control V'_{maxSi}, (correlated with ambient Fe)". Some environmental factor, irradiance in this case, then sets the "Ambient V'_{maxSi}" obtained from the station kinetic data and which has no correlation with ambient Fe. Finally, the ambient $Si(OH)_4$ uptake rate (from the station data) varies with ambient $Si(OH)_4$ concentration as required by the loss rate but shows no relation to ambient Fe. Note that each level in the cascade has a basis in observation (data) as well as in theory.

3.7. Distinguishing between limiting nutrient and factors reducing maximum uptake/growth rate

Analysis of nutrient limited continuous culture systems requires two categories of control to be recognized. First is the limiting nutrient (set up by the relationship of the mix of nutrients in the feed or source medium). The second is the environmental factor(s) limiting the maximum growth rate and thereby setting the V'_{max} for the limiting nutrient. The time scales
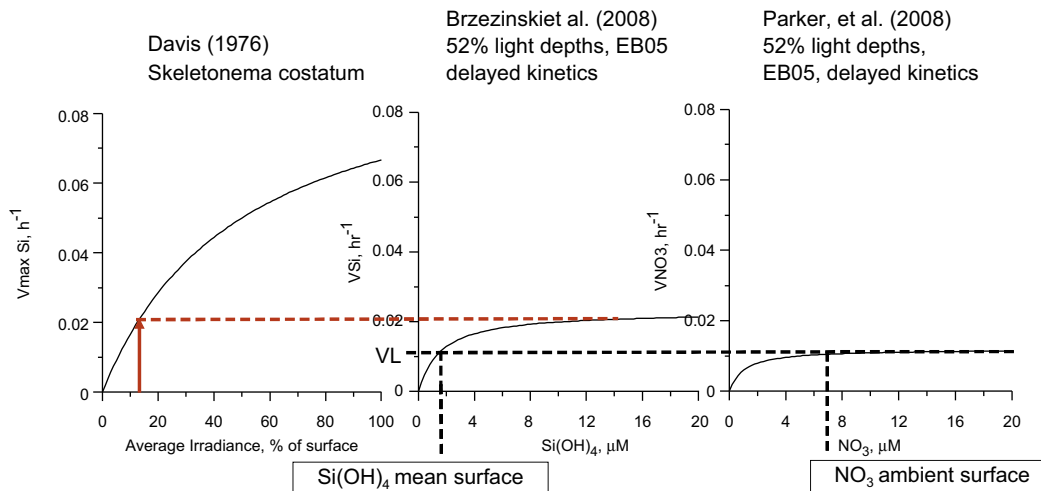

Fig. 8. Pattern of hypothetical linked limitations for equatorial Pacific diatoms. Left panel, growth limitation by ambient irradiance as shown for *Skeletonema costatum* in chemostat culture (Davis, 1976). The vertical arrow on the X axis denotes an ambient irradiance below saturation, thereby setting the V'_{maxSi}, on the V_{Si} vs. $Si(OH)_4$ hyperbola (dotted red line to center panel) measured during EB05. The loss rate, V_L (mostly grazing) sets the specific uptake rate ($=\mu$) of the limiting nutrient $Si(OH)_4$, and from the intersection of V_L with the limiting nutrient hyperbola (horizontal dotted black line), sets the ambient $Si(OH)_4$ concentration (vertical black dotted line). The value of V_L sets the specific uptake rates of NO_3 (horizontal dotted black line in right panel).
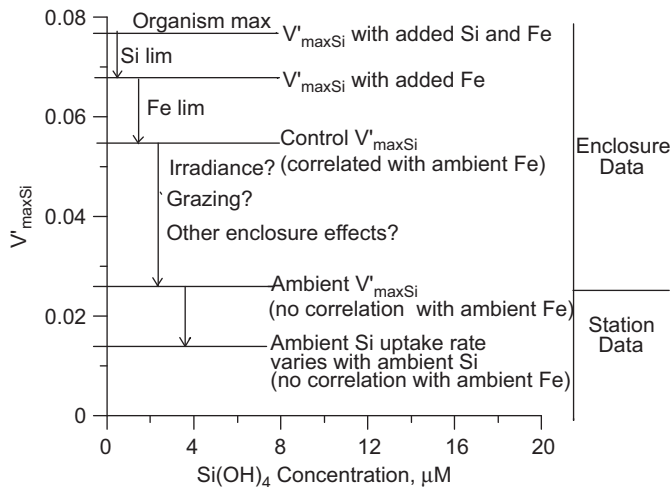
Fig. 9. Cascade of limitations on V_{maxSi} based on uptake kinetics data from stations and delayed kinetics (Brzezinski et al., 2008).

for changes in uptake rates (V'_{Si}) and growth rates (V'_{max}) rates are different. Uptake rates vary with substrate concentrations on the scale of minutes or less to hours, while changes in the growth rates or V'_{max} rates requires longer periods to adapt; days or weeks, e.g. with changes in irradiance (Davis, 1976). The maximum growth limiting factor (V'_{max}-limiting factor) should be designated in such a way as to distinguish it from the limiting nutrient. The measurements required to distinguish these two factors must be made at the appropriate time scales. The most basic factor is the limiting nutrient, e.g. $Si(OH)_4$ for the equatorial diatom system, and mean irradiance as the most likely V'_{max}-limiting factor. The limiting nutrient determines the type of nutrient uptake hyperbola and another factor sets the V'_{max} for the limiting nutrient.

The usefulness of recognizing a V'_{max} limiting factor separately from the limiting nutrient is that there can be a number of potential V'_{max} limiting factors in a system even though there will be only one limiting nutrient. The importance of distinguishing these two limitations is in understanding the changes in new production (and export production) that can occur in nutrient limited continuous productivity systems. The new production rate is set by the net flux of the limiting nutrient to the ecosystem which in turn is a function of the nutrient input (e.g. upwelling rate) and the limiting nutrient gradient between the surface and the euphotic zone. The gradient is set by the source concentration of limiting nutrient and the ambient surface limiting nutrient concentration. The surface limiting nutrient concentration is set by the interaction of the limiting nutrient hyperbola (and the loss rate, which sets the growth rate)(Fig. 5). With a constant loss rate, the growth limiting nutrient can influence the shape of the hyperbola through V'_{maxSi}, moving the ambient limiting nutrient concentration higher or lower. For example in the equatorial system, there are at least two potential factors that limit V'_{maxSi}; irradiance and Fe, both of which have been shown to determine V'_{maxSi} experimentally (Davis, 1976; Leynaert et al., 2004). Increased Fe will steepen the initial slope of the $Si(OH)_4$ uptake hyperbola and reduce the ambient (=operating) $Si(OH)_4$ concentration by a relatively small amount, $< 2 \mu M$, increasing both the source to surface concentration gradient, and diatom new production by a maximum of $< 30\%$. Reduced Fe would result eventually in a $Si(OH)_4$ hyperbola with a V'_{maxSi} approaching the ambient V'_{Si}, and as the slope changes, there will be increasing ambient $Si(OH)_4$ as predicted by Dugdale et al. (2007). The EB04 data show such an increasing ambient $Si(OH)_4$ concentration

(Fig. 10A) with decreasing Fe to the east (Fig. 10B). However, both Fe and $Si(OH)_4$ isopleths show a steep rise toward the surface at about 118°W and may be responding to some advective event. Although this analysis is based on the assumption of a steady-state condition, the reality is that perturbations occur often or continuously, but are reacted to with negative feedbacks to restore the system toward the equilibrium state. This better-termed "quasi-steady state" is attested to by the very small variability in surface $Si(OH)_4$ and chlorophyll concentrations over very large areas of the equatorial upwelling system. This quasi-steady state probably applies mostly to the near-surface, non-light limited region, while considerable changes would be expected to occur from the bottom of the euphotic zone up to the higher light regions.

3.8. Implications for equatorial new production and the role of the equatorial phytoplankton in the flux of CO_2 to the atmosphere.

The present analysis substantiates the concept of the equatorial diatom-$Si(OH)_4$ system as a quasi-chemostat regulating on $Si(OH)_4$. Several important features of the equatorial ecosystem are clarified or confirmed from these results of the EB04 and EB05 cruises. An important finding is the indication that the diatom functional group is central to the ecosystem as a primary route to the import of upwelled NO_3; i.e. up to 63% or more of new production may be diatom production (Section 3.2). Other large-sized autotrophs (e.g. dinoflagellates) may also take up NO_3 (Parker et al., 2011). Both picoplankton production and production by a non-diatom phytoplankton group that are $> 5-\mu m$ in diameter, are engaged primarily in regenerated production (NH_4 uptake). The EB04 and EB05 cruise results confirm $Si(OH)_4$ limitation of diatoms as a significant cause of high surface pCO_2 at the equator in most of the EUZ. Diatom NO_3 use and accompanying uptake of carbon (new production) will in turn be limited by the low amount of $Si(OH)_4$ in the upwelling source water (Chai et al., 2002). The result is the presence of relatively high concentrations of NO_3 and TCO_2 in equatorial surface waters. Surface NO_3 and total dissolved inorganic carbon (TCO_2) are closely linked (Fig. 11 and Dugdale et al., 2007)) as demonstrated using a meridional section across the equator at 110°W and zonal section from 110°W to 140°W that show tight linear regressions. The origin of the low $Si(OH)_4$ condition of the EUC has been traced to the Southern Ocean (Dugdale et al., 2002b; Sarmiento et al., 2004), where diatom processes result in a water mass with low $Si(OH)_4$ and high NO_3 that forms the southern half of the EUC at the western end of the Pacific. The possible effects of global change on ocean-atmosphere flux of CO_2 need to consider changes in the Southern Ocean source of nutrients that feed the equatorial $Si(OH)_4$-diatom quasi-chemostat and regulate new production of the EUZ.

4. Conclusions

This study, based on measured uptake kinetics of $Si(OH)_4$ and NO_3, and the effect of Fe on $Si(OH)_4$ uptake kinetics, supports the concept of the equatorial diatom-$Si(OH)_4$ system as a quasi-chemostat regulating on $Si(OH)_4$. No effects of Fe on $Si(OH)_4$ uptake kinetics or uptake of $Si(OH)_4$ at ambient $Si(OH)_4$ concentrations were expected from laboratory studies nor observed at the Fe concentrations encountered on the two cruises. A cascade of limitations on the maximum $Si(OH)_4$ uptake rate, essentially the diatom growth rate, was constructed reducing V'_{maxSi} in a downward order: first the effect of Fe concentration; 2) $Si(OH)_4$ concentration, 3) irradiance or some factor related to the placing of water in enclosures on-deck. The latter factor

(A)

(B)

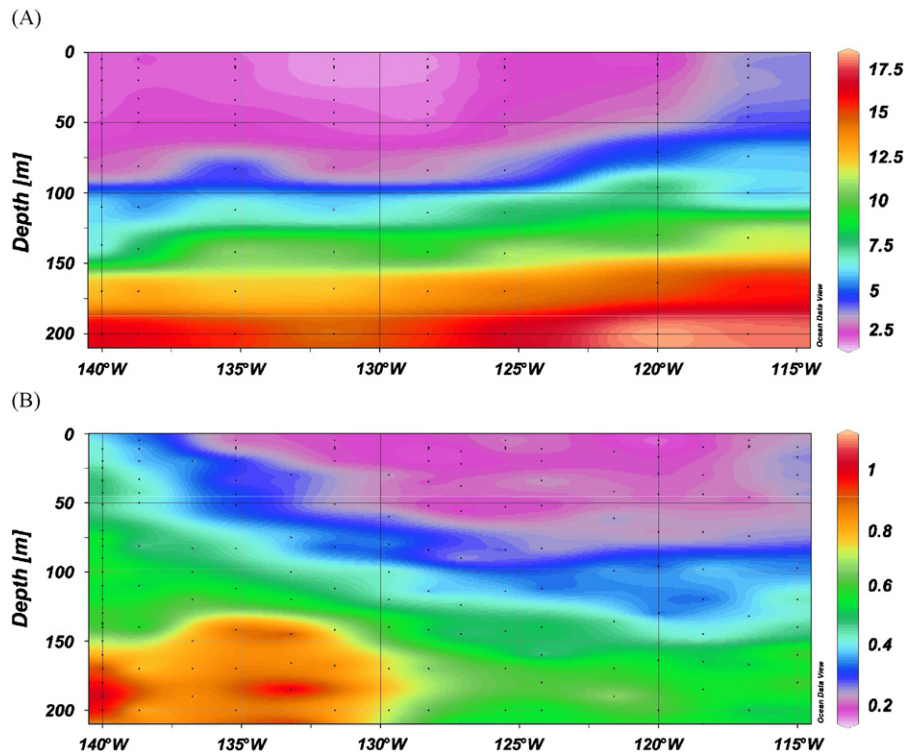
Fig. 10. Depth contoured concentrations of A) Si(OH)$_4$, μM and B) Fe, nM along the equator, EB04.
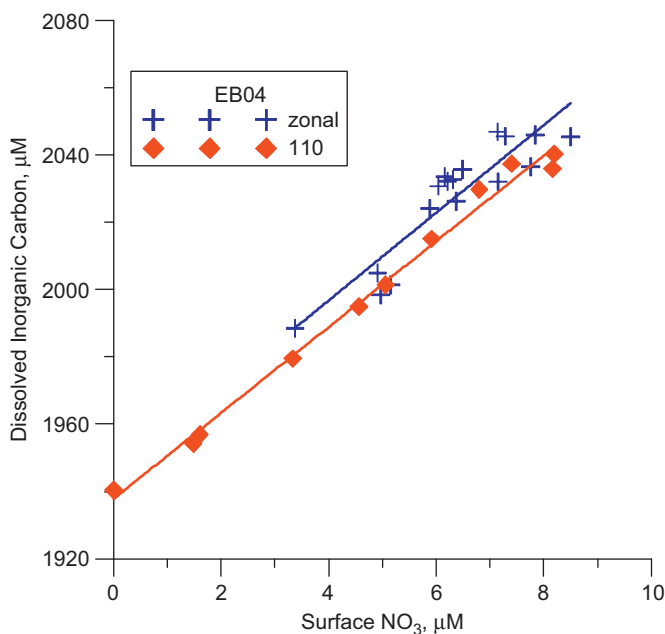

Fig. 11. Surface dissolved inorganic carbon (TCO$_2$) vs. NO$_3$ across the equator at 110°W (red triangles) and along the equator (zonal, blue crosses) during EB04, r^2=0.99 and 0.84 respectively.

appeared to be dominant for diatoms in the equatorial euphotic zone. The quasi-chemostat model also is strongly supported by the near constant level of surface Si(OH)$_4$ concentration, the varying concentration of non-limiting nutrient (i.e. NO$_3$), by the variation of Si(OH)$_4$ uptake with Si(OH)$_4$ concentration, and the low, rate of non-limiting nutrient uptake (NO$_3$ in this case) linked to the Si(OH)$_4$ uptake rate.

Diatom biomass and productivity simulated by the CoSiNE model (Chai et al., 2002) and based upon the chemostat concept agree with measured rates. These modeled and data results are based on the flux of Si(OH)$_4$ and other nutrients through the ecosystem and so lead directly to predictions of new production. The increased concentration of Si(OH)$_4$ source water between EB04 and EB05 (Parker et al, 2011, their Fig. 10) was accompanied by an increase in new production (as NO$_3$ uptake) (Table 1) and a decrease in surface NO$_3$ concentrations (predictions of CoSiNE). Regenerated production increased by a factor of 2 (Table 4), which was expected from the increased NO$_3$ uptake and low f-ratios. Finally, in agreement with De Baar et al. (2005), analysis of the EB05 station and enclosure experiments raises a caution flag when shipboard enclosure experiments are made and conclusions drawn from results of water with amendments, confined in containers and held on-deck at higher irradiance and with other changed conditions compared to the conditions they would experience *in situ*. Such conclusions should be compared with ambient *in situ* (station) data. For example, in EB05 the on-deck experimental controls were held at a higher irradiance level than the mean irradiance level being experienced by the ambient phytoplankton (at the depth that the water for the enclosures was sampled) and so were not a true control. The results provide only evidence for the ability of the phytoplankton to grow at higher rates when provided first with the improved conditions in enclosures held on-deck at 50% of surface irradiance and then even higher rates with added Fe. An additional problem arises with the assertion of a regulatory role for Fe in the equatorial system (Brzezinski et al., 2008) in that the station data fail to show any relationship between ambient Fe concentrations and Si(OH)$_4$ uptake or Si(OH)$_4$ kinetics (Fig. 6). Feynman (2000) points out that we make experiments based on theory, but data from nature tests our hypotheses. In this case, the data from nature (the measurements made of water collected at the stations) negates the hypothesis of Fe regulation (based upon carboy experiments)

of diatom productivity in the eastern equatorial Pacific upwelling zone, but supports the hypothesis of a quasi-chemostat model based on $Si(OH)_4$ limitation of diatom productivity with a high percentage of NO_3 uptake attributable to diatoms. This diatom quasi-chemostat imposes a biological element to the control of equatorial ocean-atmosphere flux of CO_2 and needs to be considered when studying global climate change.

Acknowledgments

References

Baines, S.B., Twining, B.S., Vogt, S., Balch, W.M., Fisher, N.S., Nelson, D.M., 2011. Elemental composition of equatorial Pacific diatoms exposed to additions of silicic acid and iron. Deep-Sea Research II 58 (3–4), 512–523.

Barber, R.T., 1992. Introduction to the WEC88 cruise—an investigation into why the equator is not greener. Journal of Geophysical Research 97, 609–610.

Bidigare, R.R., Chai, F., Landry, M.R., Lukas, R., Hannides, C., Christensen, S.J., Karl, D.M., Shi, L., Chao, Y., 2009. Subtropical ocean ecosystem structure changes forced by North Pacific climate variations. Journal of Plankton Research 31, 1131–1139.

Bidigare, R.R., Ondrusek, M.E., 1996. Spatial and temporal variability of phytoplankton pigment distributions in the central equatorial Pacific Ocean. Deep-Sea Research II 43, 809–833.

Blain, S., Leynaert, A., Tréguer, P., Chretiennot-Dinet, M.J., Rodier, M., 1997. Biomass, growth rates and limitation of equatorial Pacific diatoms. Deep-Sea Research I 44, 1255–1275.

Bran Luebbe AutoAnalyzer Applications, 1999. AutoAnalyzer Method No. G-177-96. Silicate in Water and Seawater. Bran Luebbe, Inc., Buffalo Grove, IL.

Brzezinski, M.A., 1985. The Si:C:N ratio of marine diatoms: interspecific variability and the effect of some environmental variables. Journal of Phycology 21, 347–357.

Brzezinski, M.A., Baines, S., Balch, W.M., Beucher, C., Chai, F., Dugdale, R.C., Krause, J.W., Landry, M.R., Marchi, A., Measures, C.I., Nelson, D.M., Parker, A., Poulton, A., Selph, K.E., Strutton, P., Taylor, A.G., Twining, B.S., 2011. Co-limitation of diatoms by iron and silicic acid in the equatorial Pacific. Deep-Sea Research II 58 (3–4), 493–511.

Brzezinski, M.A., Dumousseaud, C., Krause, J.W., Measures, C.I., Nelson, D.M., 2008. Iron and silicic acid concentrations together regulate Si uptake in the equatorial Pacific Ocean. Limnology and Oceanography 53, 875–889.

Chai, F., Dugdale, R.C., Peng, T.-H., Wilkerson, F.P., Barber, R.T., 2002. One dimensional ecosystem model of the equatorial Pacific upwelling system, Part I: model development and silicon and nitrogen cycle. Deep-Sea Research II 49, 2713–2745.

Chai, F., Jiang, M.-S., Barber, R.T., Dugdale, R.C., Chao, Y., 2003. Interdecadal variation of the transition zone chlorophyll front, a physical–biological model simulation between 1960 and 1990. Journal of Oceanography 59, 461–475.

Chai, F., Jiang, M.-S., Chao, Y., Dugdale, R.C., Chavez, F.P., Barber, R.T., 2007. Modeling responses of diatom productivity and biogenic silica export to iron enrichment in the equatorial Pacific Ocean. Global Biogeochemical Cycles, 21. doi:10.1029/2006GB002804.

Chai, F., Lindley, S.T., Barber, R.T., 1996. Origin and maintenance of a high nitrate condition in the equatorial Pacific. Deep-Sea Research II 43, 1031–1064.

Chai, F., Liu, G., Xue, H., Shi, L., Chao, Y., Tseng, C.-T., Chou, W.-C., Liu, K.-K., 2009. Seasonal and interannual variability of carbon cycle in South China Sea: a three-dimensional physical–biogeochemical modeling study. Journal of Oceanography 65, 703–720.

Coale, K.H., Johnson, K.S., Fitzwater, S.E., Gordon, R.M., Tanner, S., Hunter, C.N., Chavez, F.P., Ferioli, F.P., Sakamoto, L., Rogers, P., Millero, F., Steinberg, P., Nightingale, P., Cooper, D., Cochlan, W.P., Landry, M.R., Constantinou, J., Rollwagen, G., Trasvina, A., Kudela, R.M., 1996. A massive phytoplankton bloom induced by an ecosystems-scale fertilization experiment in the equatorial Pacific Ocean. Nature 383, 495–501.

Conway, H.L., Harrison, P.J., Davis, C.O., 1976. Marine diatoms grown in chemostats under silicate or ammonium limitation. II. Transient responses of *Skeletonema costatum* to a single addition of the limiting nutrient. Marine Biology 35, 187–199.

Davis, C.O., 1976. Continuous culture of marine diatoms under silicate limitation. II. Effect of light intensity on growth and nutrient uptake of *Skeletonema costatum*. Journal of Phycology 12, 291–300.

De Baar, H., Boyd, P., Coale, K., Landry, M., Atsushi, T., Assmy, P., Bakker, D., Bozec, Y., Barber, R., Brzezinski, M., Buesseler, K., Boyé, M., Croot, P., Gervais, F., Gorbunov, M., Harrison, F., Wiscock, W., Laan, P., Lancelot, C., Law, C., Levasseur, M., Marchetti, A., Millero, F., Nishioka, J., Nojiri, Y., van Oijen, T., Riebesell, U., Rijkenberg, M., Saito, H., Takeda, S., Timmermans, K., Veldhuis, M., Waite, A., Wong, C., 2005. Synthesis of iron fertilization experiments: from the iron age in the age of enlightenment. Journal of Geophysical Research 110, C09S16. doi:10.1029/2004JC002601.

Demarest, M.S., Brzezinski, M.A., Nelson, D.M., Krause, J.W., Jones, J.L., Beucher C., 2011. Net biogenic silica production and nitrate regeneration determine the strength of the silica pump in the eastern equatorial Pacific. Deep Sea Research II 58 (3–4), 462–476.

Dugdale, R.C., 1967. Nutrient limitation in the sea: dynamics, identification, and significance. Limnology and Oceanography 12, 685–695.

Dugdale, R.C., Goering, J.J., 1967. Uptake of new and regenerated forms of nitrogen in primary productivity. Limnology and Oceanography 12, 196–206.

Dugdale, R.C., Jones, B.H., MacIsaac J.J., Goering, J.J., 1981. Adaptation of nutrient assimilation. In: Platt, T. (Ed.), Canadian Bulletin of Fisheries and Agriculture Sciences 210, pp. 234–250.

Dugdale, R.C., Wilkerson, F.P., 1986. The use of N-15 to measure nitrogen uptake in eutrophic oceans—experimental considerations. Limnology and Oceanography 31, 673–689.

Dugdale, R.C., Wilkerson, F.P., 1998. Silicate regulation of new production in the equatorial Pacific upwelling. Nature 391, 270–273.

Dugdale, R.C., Wilkerson, F.P., Minas, H.J., 1995. The role of a silicate pump in driving new production. Deep-Sea Research 42, 697–719.

Dugdale, R.C., Wilkerson, F.P., Chai, F., Feely, R., 2007. Size fractionated nitrogen uptake measurements in the equatorial Pacific and confirmation of the low Si-high nutrient low chlorophyll condition. Global Biogeochemical Cycles 21 (2), GB2005. doi:10.1029/2006GB002722.

Dugdale, R.C., Barber, R.T., Chai, F., Peng, T.H., Wilkerson, F.P., 2002a. One dimensional ecosystem model of the equatorial Pacific upwelling system, Part II: sensitivity analysis and comparison with JGOFS EqPac data. Deep-Sea Research II 49, 2747–2768.

Dugdale, R.C., Wischmeyer, A.G., Wilkerson, F.P., Barber, R.T., Chai, F., Jiang, M., Peng, T.-H., 2002b. Meridional asymmetry of source nutrients to the equatorial Pacific upwelling ecosystem and it's potential impact on ocean-atmosphere CO_2 flux; a data and modeling approach. Deep-Sea Research II 49, 2513–2533.

Feely, R.A., Wanninkhof, R., Takahashi, T., Tans, P., 1999a. Influence of El Niño on the equatorial Pacific contribution of atmospheric CO_2 accumulation. Nature 398, 597–601.

Feely, R.A., Lamb, M.F., Greeley, D.J., Wanninkhof, R., 1999b. Comparison of the carbon system parameters at the global CO_2 survey crossover locations in the North and South Pacific Ocean, 1990–1996, ORNL/CDIAC-115. Carbon Dioxide Information Analysis Center, Oak Ridge National Laboratory, U.S. Department of Energy, Oak Ridge, Tenn. 74pp.

Feynman, R., 2000. The Pleasure of Finding Things Out. Da Capo Press 270pp.

Frost, B.W., Franzen, N.C., 1992. Grazing and iron limitation in the control of phytoplankton stock and nutrient concentration: a chemostat analogue of the Pacific equatorial upwelling zone. Marine Ecology Progress Series 83, 291–303.

Fujii, M., Chai, F., 2009. Influences of initial plankton biomass and mixed-layer depths on the outcome of iron-fertilization experiments. Deep-Sea Research II. doi:10.1016/j.dsr2.2009.07.007.

Harrison, P.J., Conway, H.L., Dugdale, R.C., 1976. Marine diatoms grown in chemostats under silicate or ammonium limitation. I. Cellular chemical composition and steady-state growth kinetics of *Skeletonema costatum*. Marine Biology 35, 177–186.

Jiang, M.-S., Chai, F., 2005. Physical and biological controls on the latitudinal asymmetry of surface nutrients and pCO₂ in the central and eastern equatorial Pacific. Journal of Geophysical Research 110, C06007.

Jiang, M.-S., Chai, F., 2006. Physical control on the seasonal cycle of surface pCO₂ in the equatorial Pacific. Geophysical Research Letters 33, L23608. doi:10.1029/2006GL02719.

Jiang, M-S., Chai, F., Dugdale, R.C., Wilkerson, F.P., Peng, T-H., Barber, R.T., 2003. A nitrate and silicate budget in the equatorial Pacific Ocean: a coupled physical-biological model study. Deep-Sea Research II, 50, 2971–2996.

Kaupp, L.J., Measures, C.I., Selph, K.E., Mackenzie, F.T., 2011. The distribution of dissolved Fe and Al in the upper waters of the eastern equatorial Pacific. Deep-Sea Research II 58 (3–4), 296–310.

Krause, J.W., Nelson, D.M., Brzezinski, M.A., 2011. Biogenic silica production and the diatom contribution to primary production and nitrate uptake in the eastern equatorial Pacific Ocean. Deep-Sea Research II 58 (3–4), 434–448.

Ku, T.-L., Luo, S., Kusakabe, M., Bishop, J.K.B., 1995. ²²⁸Ra-derived nutrient budgets in the upper equatorial Pacific and the role of "new" silicate in limiting productivity. Deep-Sea Research II 42, 479–497.

Leynaert, A., Bucciarelli, E., Claquin, P., Dugdale, R.C., Martin-Jézéquel, V., Pondaven, P., Ragueneau, O., 2004. Effect of iron deficiency on diatom cell size and silicic acid uptake kinetics. Limnology and Oceanography 49, 1134–1143.

Leynaert, A., Tréguer, P., Lancelot, C., Rodier, M., 2001. Silicon limitation of biogenic silica production in the equatorial Pacific. Deep-Sea Research I 48, 639–660.

Measures, C.I., Yuan, J., Resing, J.A., 1995. Determination of iron in seawater by flow injection analysis using in-line preconcentration and spectrophotometric detection. Marine Chemistry 50, 3–12.

Minas, H.J., Minas, M., 1992. Net community production in "high nutrient–low chlorophyll" waters of the tropical and Antarctic Oceans: grazing vs. iron hypothesis. Oceanologica Acta 15, 145–162.

Murray, J.W. (Guest Ed.), 1995. A U.S. JGOFS process study in the equatorial Pacific. Deep-Sea Research II 42, 275–902.

Murray, J.W. (Guest Ed.), 1996. A U.S. JGOFS process study in the equatorial Pacific. Part 2. Deep-Sea Research II 43.

Murray, J.W., LeBorgne, R., Dandonneau, Y., 1997. JGOFS studies in the equatorial Pacific. Deep-Sea Research II 44, 1759–1763.

Palacz, A.P., Chai, F., Dugdale, R.C., Measures, C.I., 2011. Estimating iron and aluminum removal rates in the eastern equatorial Pacific Ocean using a box model approach. Deep-Sea Research II 58 (3–4), 311–324.

Parker, A.E., Wilkerson, F.P., Dugdale, R.C., Marchi, A., Hogue, V.E., Landry, M.R., Taylor, A.G., 2011. Spatial patterns of nitrogen uptake and phytoplankton in the equatorial upwelling zone (110°W–140°W) during 2004 and 2005. Deep-Sea Research II 58 (3–4), 417–433.

Rodier, M., LeBorgne, R., 1997. Export flux of particles at the equator in the western and central Pacific Ocean. Deep-Sea Research II 44, 2085–2113.

Sarmiento, J.L., Gruber, N., Brzezinski, M., Dunne., J.P., 2004. High-latitude controls of thermocline nutrients and low latitude biological productivity. Nature 427, 56–60.

Solorzano, L., 1969. Determination of ammonia in natural waters by the phenolhypochlorite method. Limnology and Oceanography 14, 799–801.

Takahashi, T., Sutherland, S.C., Sweeney, C., Poisson, A., Metz, N., Tilbrook, B., Bates, N., Wanninkhof, R., Feely, R.A., Sabine, C., Olafssong, J., Nojiri, Y., 2002. Global sea–air CO_2 flux based on climatological surface ocean pCO_2, and seasonal biological and temperature effects. Deep-Sea Research II 49, 1601–1622.

Taylor, A.G., Landry, M.R., Selph, K., Yang, E-J., 2011. Biomass, size structure and depth distributions of the microbial community in the eastern equatorial Pacific. Deep-Sea Research II 58 (3–4), 342–357.

Walter, C., 1965. Steady State Applications in Enzyme Kinetics. The Ronald Press Company, NY 262pp.

Whitledge, T.E., Malloy, S., Patton, C.J., Wirick, C.D., 1981. Automated nutrient analysis in seawater. Technical Report BNL 51398. Brookhaven National Laboratory 226pp.

Wilkerson, F.P., Dugdale, R.C., 1992. Measurements of nitrogen productivity in the equatorial Pacific. Journal of Geophysical Research 97, 669–679.